Resonant and Near-Resonant Internal Wave Interactions

AUTHOR(S):

Lvov, Yuri V.; Polzin, Kurt L.; Yokoyama, Naoto

CITATION:

Lvov, Yuri V. ...[et al]. Resonant and Near-Resonant Internal Wave Interactions. Journal of Physical Oceanography 2012, 42(5): 669-691

ISSUE DATE:

2012-05

URL:

http://hdl.handle.net/2433/193707

Resonant and Near-Resonant Internal Wave Interactions

YURI V. LVOV

Department of Mathematical Sciences, Rensselaer Polytechnic Institute, Troy, New York

KURT L. POLZIN

Woods Hole Oceanographic Institution, Woods Hole, Massachusetts

NAOTO YOKOYAMA

Department of Aeronautics and Astronautics, Kyoto University, Kyoto, Japan

(Manuscript received 19 August 2008, in final form 25 March 2011)

ABSTRACT

The spectral energy density of the internal waves in the open ocean is considered. The Garrett and Munk spectrum and the resonant kinetic equation are used as the main tools of the study. Evaluations of a resonant kinetic equation that suggest the slow time evolution of the Garrett and Munk spectrum is not in fact slow are reported. Instead, nonlinear transfers lead to evolution time scales that are smaller than one wave period at high vertical wavenumber. Such values of the transfer rates are inconsistent with the viewpoint expressed in papers by C. H. McComas and P. Müller, and by P. Müller et al., which regards the Garrett and Munk spectrum as an approximate stationary state of the resonant kinetic equation. It also puts the self-consistency of a resonant kinetic equation at a serious risk. The possible reasons for and resolutions of this paradox are explored. Inclusion of near-resonant interactions decreases the rate at which the spectrum evolves. Consequently, this inclusion shows a tendency of improving of self-consistency of the kinetic equation approach.

1. Introduction

Wave–wave interactions in stratified oceanic flows have been a fascinating subject of research in the last four decades. Of particular importance is the existence of a ''universal'' internal wave spectrum, the Garrett and Munk (GM; Garrett and Munk 1972, 1975, 1979) spectrum. It is generally perceived that the existence of a universal spectrum is, at least in part and perhaps even primarily, the result of nonlinear interactions of waves with different wavenumbers. Because of the quadratic nonlinearity of the underlying primitive equations and the fact that the linear internal wave dispersion relation can satisfy a three-wave resonance condition, waves interact in triads. Therefore, the question arises, how strongly do waves within a given triad interact? What are the oceanographic consequences of this interaction?

Wave–wave interactions can be rigorously characterized by deriving a closed equation representing the slow time evolution of the wave field's wave action spectrum. Such an equation is called a kinetic equation (Zakharov et al. 1992), and significant efforts in this regard are listed in Table 1.

A kinetic equation describes, under the assumption of weak nonlinearity, the resonant spectral energy transfer on the resonant manifold. The resonant manifold is a set of wave vectors $\mathbf{p}$, $\mathbf{p}_1$, and $\mathbf{p}_2$ that satisfy

$$\mathbf{p} = \mathbf{p}_1 + \mathbf{p}_2, \quad \omega_{\mathbf{p}} = \omega_{\mathbf{p}_1} + \omega_{\mathbf{p}_2}, \tag{1}$$

where the frequency ω is given by a linear dispersion relation relating wave frequency ω with wavenumber $\mathbf{p}$.

The reduction of all possible interactions between three wave vectors to a resonant manifold is a significant simplification. Even further simplification can be achieved by taking into account that, of all interactions on the resonant manifold, the most important are those that involve extreme scale separations (McComas and Bretherton 1977) between interaction wave vectors. It is shown in

Corresponding author address: Yuri V. Lvov, Department of Mathematical Sciences, Rensselaer Polytechnic Institute, Troy, NY 12180.
E-mail: lvovy@rpi.edu

DOI: 10.1175/2011JPO4129.1

TABLE 1. A list of various kinetic equations. Results from Olbers (1976), McComas and Bretherton (1977), and Pomphrey et al. (1980) are reviewed in Müller et al. (1986), who state that Olbers (1976), McComas and Bretherton (1977), and an unspecified Eulerian representation are consistent on the resonant manifold. Pomphrey et al. (1980) utilizes Langevin techniques to assess nonlinear transports. Müller et al. (1986) characterizes those Langevin results as being mutually consistent with the direct evaluations of kinetic equations presented in Olbers (1976) and McComas and Bretherton (1977). Kenyon (1968) states (without detail) that Kenyon (1966) and Hasselmann (1966) give numerically similar results. A formulation in terms of discrete modes will typically permit an arbitrary buoyancy profile, but obtaining results requires specification of the profile. Of the discrete formulations, Pomphrey et al. (1980) use an exponential profile and the others assume a constant stratification rate.

Source	Coordinate system	Vertical structure	Rotation	Hydrostatic	Special
Hasselmann (1966)	Lagrangian	Discrete	No	No	
Kenyon (1966, 1968)	Eulerian	Discrete	No	No	Non Hamiltonian
Müller and Olbers (1975)[a]	Lagrangian	Continuous	Yes	No	
McComas (1975, 1977)	Lagrangian	Continuous	Yes	Yes	
Pelinovsky and Raevsky (1977)	Lagrangian	Continuous	No	No	Clebsch
Voronovich (1979)[b]	Eulerian	Continuous	No	Yes	Clebsch
Pomphrey et al. (1980)	Lagrangian	Discrete	Yes	No	Langevin
Milder (1982)	isopycnal	—	No	No	
Caillol and Zeitlin (2000)[b]	Eulerian	Continuous	No	No	Non Hamiltonian
Lvov and Tabak (2001)[b]	Isopycnal	Continuous	No	Yes	Canonical
Lvov and Tabak (2004)[c]	Isopycnal	Continuous	Yes	Yes	Canonical

[a] This kinetic equation is investigated in sections 3, 4, and the appendix.
[b] This kinetic equation is investigated in section 3.
[c] This kinetic equation is investigated in sections 3, 4, 5, and the appendix.

McComas (1977) that the high-frequency portion of the Garrett and Munk internal wave spectrum is stationary with respect to one class of such interactions, called induced diffusion (ID). Furthermore, a comprehensive inertial-range theory with constant downscale transfer of energy was obtained by patching these mechanisms together in a solution that closely mimics the empirical universal spectrum (GM) (McComas and Müller 1981a). It was therefore concluded that that Garrett and Munk spectrum constitutes an approximate stationary state of the kinetic equation.

In this paper, we revisit the question of relation between Garrett and Munk spectrum and the resonant kinetic equation. At the heart of this paper (section 6a) are numerical evaluations of the Lvov and Tabak (2004) internal wave kinetic equation demonstrating changes in spectral amplitude at a rate greater than an inverse wave period at high vertical wavenumber for the Garrett and Munk spectrum. This rapid temporal evolution implies that the GM spectrum is not a stationary state and is contrary to the characterization of the GM spectrum as an inertial subrange. This result gave us cause to review published work concerning wave–wave interactions and compare results. The product of this work is presented in sections 3 and 4. In particular, we concentrate on four different versions of the internal wave kinetic equation:

- a noncanonical description using Lagrangian coordinates (Olbers 1974, 1976; Müller and Olbers 1975),
- a canonical Hamiltonian description in Eulerian coordinates (Voronovich 1979),
- a dynamical derivation of a kinetic equation without use of Hamiltonian formalisms in Eulerian coordinates (Caillol and Zeitlin 2000), and
- a canonical Hamiltonian description in isopycnal coordinates (Lvov and Tabak 2001, 2004).

We show in section 3 that, without background rotation, all the listed approaches are equivalent on the resonant manifold. In section 4, we demonstrate that the two versions of the kinetic equation that consider nonzero rotation rates are again equivalent on the resonant manifold. This presents us with our first paradox: if all these kinetic equations are the same on the resonant manifold and exhibit a rapid temporal evolution, then why is GM considered to be a stationary state? The resolution of this paradox, presented in section 7, is that (i) numerical evaluations of the McComas (1977) kinetic equation demonstrating the induced diffusion stationary states require damping in order to balance the rapid temporal evolution at high vertical wavenumber and (ii) the high-wavenumber temporal evolution of the Lvov and Tabak (2004) kinetic equation is tentatively identified as being associated with the elastic scattering (ES) mechanism rather than induced diffusion.

Having clarified this, we proceed to the following observation: Not only do our numerical evaluations imply that the GM spectrum is not a stationary state, the rapid evolution rates correspond to a strongly nonlinear system. Consequently, the self-consistency of the kinetic equation, which is built on an assumption of weak nonlinearity, is at risk. Moreover, reduction of all resonant wave–wave

interactions exclusively to extreme scale separations is also not self-consistent.

However, we are not willing to give up on the kinetic equation. Our second paradox is that, in a companion paper (Lvov et al. 2010), we show how a comprehensive theory built on a scale-invariant resonant kinetic equation helps to interpret the observed variability of the background oceanic internal wave field. The observed variability, in turn, is largely consistent with the induced diffusion mechanism being a stationary state.

Thus, the resonant kinetic equation demonstrates promising predictive ability, and it is therefore tempting to move toward a self-consistent wave turbulence theory of internal waves. One possible route toward such theory is to include to the kinetic equation near-resonant interactions, defined as

$$\mathbf{p} = \mathbf{p}_1 + \mathbf{p}_2, \quad |\omega_{\mathbf{p}} - \omega_{\mathbf{p}_1} - \omega_{\mathbf{p}_2}| < \Gamma,$$

where Γ is the resonance width. We show in section 6b that such resonant broadening leads to slower evolution rates, potentially leading to a more self-consistent description of internal waves.

We conclude and list open questions in section 8. Our numerical scheme for evaluating near-resonant interactions is discussed in section 5. An appendix contains the interaction matrices used in this study.

2. Background

A kinetic equation is a closed equation for the time evolution of the wave action spectrum in a system of weakly interacting waves. It is usually derived as a central result of wave turbulence theory. The concepts of wave turbulence theory provide a fairly general framework for studying the statistical steady states in a large class of weakly interacting and weakly nonlinear many-body or many-wave systems. In its essence, classical wave turbulence theory (Zakharov et al. 1992) is a perturbation expansion in the amplitude of the nonlinearity, yielding, at the leading order, linear waves, with amplitudes slowly modulated at higher orders by resonant nonlinear interactions. This modulation leads to a redistribution of the spectral energy density among space and time scales.

Although the route to deriving the spectral evolution equation from wave amplitude is fairly standardized (section 2b), there are substantive differences in obtaining expressions for the evolution equations of wave amplitude a. Section 2a describes how it is done in isopycnal coordinates in Lvov and Tabak (2001, 2004) and in the appendix for all other methods discussed in the present paper.

a. *Hamiltonian structures and field variables in isopycnal coordinates*

Lvov and Tabak (2001, 2004) start from the primitive equations of motion written in isopycnal coordinates,

$$\begin{aligned} \frac{\partial}{\partial t}\frac{\partial z}{\partial \rho} + \nabla \cdot \left(\frac{\partial z}{\partial \rho}\mathbf{u}\right) &= 0, \\ \frac{\partial \mathbf{u}}{\partial t} + f\mathbf{u}^{\perp} + \mathbf{u}\cdot\nabla\mathbf{u} + \frac{\nabla M}{\rho_0} &= 0, \\ \frac{\partial M}{\partial \rho} - gz &= 0, \end{aligned} \tag{2}$$

representing mass conservation, horizontal momentum conservation under the Boussinesq approximation, and hydrostatic balance. The velocity $\mathbf{u}$ is then represented as (Lelong and Riley 1992, 2000)

$$\mathbf{u} = \nabla\phi + \nabla^{\perp}\psi,$$

with $\nabla^{\perp} = (-\partial/\partial y, \partial/\partial x)$, and a normalized differential layer thickness is introduced,

$$\Pi = (\rho_0/g)\partial^2 M/\partial\rho^2 = \rho_0 \partial z/\partial\rho. \tag{3}$$

Because both potential vorticity and density are conserved along particle trajectories, an initial profile of the potential vorticity that is a function of the density will be preserved by the flow. Hence it is self-consistent to assume that the potential vorticity q is function of ρ only, independent of x and y,

$$q(\rho) = q_0(\rho) = \frac{f}{\Pi_0(\rho)}, \tag{4}$$

where $\Pi_0(\rho) = -g/N(\rho)^2$ is a reference stratification profile with background buoyancy frequency, $N = [-g/(\rho\partial z/\partial\rho|_{\mathrm{bg}})]^{1/2}$, independent of x and y. The variable ψ can then be eliminated by assuming that potential vorticity is constant on an isopycnal so that $f + \Delta\psi = q_0\Pi$ and one obtains two equations in Π and ϕ,

$$\begin{aligned} \Pi_t + \nabla\cdot\{\Pi[\nabla\phi + \nabla^{\perp}\Delta^{-1}(q_0\Pi - 1)]\} &= 0, \\ \phi_t + \frac{1}{2}|\nabla\phi + \nabla^{\perp}\Delta^{-1}(q_0\Pi - 1)|^2 + \Delta^{-1}\nabla\cdot\{q_0\Pi[\nabla^{\perp}\phi \\ - \nabla\Delta^{-1}(q_0\Pi - 1)]\} + \frac{g}{\rho_0^2}\int^{\rho}\int^{\rho'}\frac{\Pi - \Pi_0}{\rho_1}d\rho_1\, d\rho' &= 0. \end{aligned} \tag{5}$$

Here, Δ^{-1} is the inverse Laplacian and ρ' represents a variable of integration rather than perturbation. Serendipitously, the variable Π is the canonical conjugate of ϕ,

$$\frac{\partial \Pi}{\partial t} = \frac{\delta \mathcal{H}}{\delta \phi}, \quad \frac{\partial \phi}{\partial t} = -\frac{\delta \mathcal{H}}{\delta \Pi}, \tag{6}$$

under a Hamiltonian $\mathcal{H}$,

$$\mathcal{H} = \int d\mathbf{x}\, d\rho \left\{ -\frac{1}{2}[\Pi_0 + \Pi(\mathbf{x},\rho)] \left| \nabla \phi(\mathbf{x},\rho) + \frac{f}{\Pi_0} \nabla^{\perp} \Delta^{-1} \Pi(\mathbf{x},\rho) \right|^2 + \frac{g}{2} \left| \int^{\rho} d\rho' \frac{\Pi(\mathbf{x},\rho')}{\rho_0} \right|^2 \right\}, \tag{7}$$

that is the sum of kinetic and potential energies.

Switching to Fourier space and introducing a complex field variable $a_{\mathbf{p}}$ through the transformation

$$\phi_{\mathbf{p}} = \frac{iN\sqrt{\omega_{\mathbf{p}}}}{\sqrt{2g|\mathbf{k}|}}(a_{\mathbf{p}} - a^*_{-\mathbf{p}}),$$
$$\Pi_{\mathbf{p}} = \Pi_0 - \frac{N\Pi_0|\mathbf{k}|}{\sqrt{2g\omega_{\mathbf{p}}}}(a_{\mathbf{p}} + a^*_{-\mathbf{p}}), \tag{8}$$

where the frequency ω satisfies the linear dispersion relation

$$\omega_{\mathbf{p}} = \sqrt{f^2 + \frac{g^2}{\rho_0^2 N^2}\frac{|\mathbf{k}|^2}{m^2}}, \tag{9}$$

the equations of motion (3) adopt the canonical form

$$i\frac{\partial}{\partial t} a_{\mathbf{p}} = \frac{\delta \mathcal{H}}{\delta a^*_{\mathbf{p}}}, \tag{10}$$

with the Hamiltonian

$$\mathcal{H} = \int d\mathbf{p}\, \omega_{\mathbf{p}} |a_{\mathbf{p}}|^2 + \int d\mathbf{p}_{012}[\delta_{\mathbf{p}+\mathbf{p}_1+\mathbf{p}_2}(U_{\mathbf{p},\mathbf{p}_1,\mathbf{p}_2} a^*_{\mathbf{p}} a^*_{\mathbf{p}_1} a^*_{\mathbf{p}_2} + \text{c.c.}) + \delta_{-\mathbf{p}+\mathbf{p}_1+\mathbf{p}_2}(V^{\mathbf{p}}_{\mathbf{p}_1,\mathbf{p}_2} a^*_{\mathbf{p}} a_{\mathbf{p}_1} a_{\mathbf{p}_2} + \text{c.c.})]. \tag{11}$$

Equation (10) is Hamilton's equation and (11) is the standard form of the Hamiltonian of a system dominated by three-wave interactions (Zakharov et al. 1992). Calculations of interaction coefficients U and V are a tedious but straightforward task, completed in Lvov and Tabak (2001, 2004). The result of this calculation is also presented in the appendix in Eq. (A21).

We emphasize that (10) is, with simply a Fourier decomposition and assumption of uniform potential vorticity on an isopycnal, precisely equivalent to the fully nonlinear equations of motion in isopycnal coordinates (2). All other formulations of an internal wave kinetic equation considered here depend upon a linearization prior to the derivation of the kinetic equation via an assumption of weak nonlinearity.

The difficulty is that, in order to utilize Hamilton's equation (10), the Hamiltonian (7) must first be constructed as a function of the generalized coordinates and momenta (Π and ϕ here). It is not always possible to do so directly, in which case one must set up the associated Lagrangian ($\mathcal{L}$ in the appendix) and then calculate the generalized coordinates and momenta.

b. *Wave turbulence*

Here, we derive the kinetic equation following Zakharov et al. (1992). We introduce wave action as

$$n_{\mathbf{p}} = \langle a^*_{\mathbf{p}} a_{\mathbf{p}} \rangle, \tag{12}$$

where $n_{\mathbf{p}} = n(\mathbf{p})$ is a three-dimensional wave action spectrum (spectral energy density divided by frequency) and the interacting wave vectors $\mathbf{p}$, $\mathbf{p}_1$, and $\mathbf{p}_2$ are given by

$$\mathbf{p} = (\mathbf{k}, m)$$

(i.e., $\mathbf{k}$ is the horizontal part of $\mathbf{p}$ and m is its vertical component). Furthermore, $\langle \cdots \rangle$ indicates the averaging over the statistical ensemble of many realizations of the internal waves.

To derive the time evolution of $n_{\mathbf{p}}$ we multiply the amplitude equation (10) with the Hamiltonian given by (11) by $a^*_{\mathbf{p}}$ and then multiply the conjugate of this equation by $a_{\mathbf{p}}$. We then subtract the two equations and average $\langle \cdots \rangle$ the result. We get

$$\frac{\partial n_{\mathbf{p}}}{\partial t} = \Im \int [V^{\mathbf{p}}_{\mathbf{p}_1\mathbf{p}_2} J^{\mathbf{p}}_{\mathbf{p}_1\mathbf{p}_2} \delta(\mathbf{p} - \mathbf{p}_1 - \mathbf{p}_2) - V^{\mathbf{p}_2}_{\mathbf{p}\mathbf{p}_1} J^{\mathbf{p}_2}_{\mathbf{p}\mathbf{p}_1} \delta(\mathbf{p}_2 - \mathbf{p} - \mathbf{p}_1) - V^{\mathbf{p}_1}_{\mathbf{p}\mathbf{p}_2} J^{\mathbf{p}_1}_{\mathbf{p}\mathbf{p}_2} \delta(\mathbf{p}_1 - \mathbf{p}_2 - \mathbf{p})]\, d\mathbf{p}_1 d\mathbf{p}_2, \tag{13}$$

where $\Im$ denotes the imaginary part, and we introduced a triple correlation function,

$$J^{\mathbf{p}}_{\mathbf{p}_1\mathbf{p}_2} \delta(\mathbf{p}_1 - \mathbf{p} - \mathbf{p}_2) \equiv \langle a^*_{\mathbf{p}} a_{\mathbf{p}_1} a_{\mathbf{p}_2} \rangle. \tag{14}$$

If we were to have noninteracting fields (i.e., fields with $V^{\mathbf{p}}_{\mathbf{p}_1\mathbf{p}_2}$ being zero), this triple correlation function would be zero. We then use perturbation expansion in smallness of interactions to calculate the triple correlation at first

order. The first-order expression for $\partial n_{\mathbf{p}}/\partial t$ therefore requires computing $\partial J^{\mathbf{p}}_{\mathbf{p}_1\mathbf{p}_2}/\partial t$ to first order. To do so we take definition (14) and use (10) with Hamiltonian (11) and apply $\langle\cdots\rangle$ averaging. We get

$$\left[i\frac{\partial}{\partial t} + (\omega_{\mathbf{p}_1} - \omega_{\mathbf{p}_2} - \omega_{\mathbf{p}_3})\right] J^{\mathbf{p}_1}_{\mathbf{p}_2\mathbf{p}_3} = \int\left[-\frac{1}{2}(V^{\mathbf{p}_1}_{\mathbf{p}_4\mathbf{p}_5})^* J^{\mathbf{p}_4\mathbf{p}_5}_{\mathbf{p}_2\mathbf{p}_3}\delta(\mathbf{p}_1 - \mathbf{p}_4 - \mathbf{p}_5) + (V^{\mathbf{p}_4}_{\mathbf{p}_2\mathbf{p}_5})^* J^{\mathbf{p}_1\mathbf{p}_5}_{\mathbf{p}_3\mathbf{p}_4}\delta(\mathbf{p}_4 - \mathbf{p}_2 - \mathbf{p}_5) + V^{\mathbf{p}_4}_{\mathbf{p}_3\mathbf{p}_5} J^{\mathbf{p}_1\mathbf{p}_5}_{\mathbf{p}_2\mathbf{p}_4}\delta(\mathbf{p}_4 - \mathbf{p}_3 - \mathbf{p}_5)\right] d\mathbf{p}_4\, d\mathbf{p}_5. \tag{15}$$

Here we introduced the quadruple correlation function

$$J^{\mathbf{p}_1\mathbf{p}_2}_{\mathbf{p}_3\mathbf{p}_4}\delta(\mathbf{p}_1 + \mathbf{p}_2 - \mathbf{p}_3 - \mathbf{p}_4) \equiv \langle a^*_{\mathbf{p}_1} a^*_{\mathbf{p}_1} a_{\mathbf{p}_3} a_{\mathbf{p}_4}\rangle. \tag{16}$$

The next step is to assume Gaussian statistics and to express $J^{\mathbf{p}_1\mathbf{p}_2}_{\mathbf{p}_3\mathbf{p}_4}$ as a product of two two-point correlators as

$$J^{\mathbf{p}_1\mathbf{p}_2}_{\mathbf{p}_3\mathbf{p}_4} = n_{\mathbf{p}_1} n_{\mathbf{p}_2}[\delta(\mathbf{p}_1 - \mathbf{p}_3)\delta(\mathbf{p}_2 - \mathbf{p}_4) + \delta(\mathbf{p}_1 - \mathbf{p}_4)\delta(\mathbf{p}_2 - \mathbf{p}_3)].$$

Then,

$$\left[i\frac{\partial}{\partial t} + (\omega_{\mathbf{p}_1} - \omega_{\mathbf{p}_2} - \omega_{\mathbf{p}_3})\right] J^{\mathbf{p}_1}_{\mathbf{p}_2\mathbf{p}_3} = (V^{\mathbf{p}_1}_{\mathbf{p}_2\mathbf{p}_3})^*(n_1 n_3 + n_1 n_2 - n_2 n_3). \tag{17}$$

Time integration of the equation for $J^{\mathbf{p}_1}_{\mathbf{p}_2\mathbf{p}_3}$ will contain fast oscillations due to the initial value of $J^{\mathbf{p}_1}_{\mathbf{p}_2\mathbf{p}_3}$ and slow evolution due to the nonlinear wave interactions. Contribution from the first term will rapidly decrease with time, so we neglect these terms. We also add infinitesimal damping to the waves linear dispersion relation to take into account dissipation effects in the system,[1]

$$\omega_{\mathbf{p}} \to \omega_p + i\tilde{\gamma}_p. \tag{18}$$

The result is given by

$$J^{\mathbf{p}_1}_{\mathbf{p}_2\mathbf{p}_3} = \frac{(V^{\mathbf{p}_1}_{\mathbf{p}_2\mathbf{p}_3})^*(n_1 n_3 + n_1 n_2 - n_2 n_3)}{\omega_{\mathbf{p}_1} - \omega_{\mathbf{p}_2} - \omega_{\mathbf{p}_3} + i\tilde{\Gamma}_{\mathbf{p}_1\mathbf{p}_2\mathbf{p}_3}}, \tag{19}$$

where we introduced the nonlinear damping of the triads of waves $\tilde{\Gamma}_{\mathbf{p}_1\mathbf{p}_2\mathbf{p}_3}$ as

$$\tilde{\Gamma}_{\mathbf{p}_1\mathbf{p}_2\mathbf{p}_3} = \tilde{\gamma}_{p_1} + \tilde{\gamma}_{p_2} + \tilde{\gamma}_{p_3}. \tag{20}$$

The physical interpretation of this formula is that the total width of the resonance is the sum of individual widths of each frequency. The width of each frequency is directly related to the damping of that frequency, as in the case of the simple harmonic oscillator. We will return to this question in more detail in section 5a.

We now substitute (19) into (13) and take a limit of $\tilde{\Gamma}_{\mathbf{p}_1\mathbf{p}_2\mathbf{p}_3} \to 0$ (i.e., assume for now that the damping of the wave is small[2]), and we use

$$\lim_{\tilde{\Gamma}\to 0} \Im\left[\frac{1}{\epsilon + i\tilde{\Gamma}}\right] = -\pi\delta(\epsilon). \tag{21}$$

We then obtain the three-wave kinetic equation (Zakharov et al. 1992; Lvov and Nazarenko 2004; Lvov et al. 1997),

$$\frac{dn_{\mathbf{p}}}{dt} = 4\pi\int|V^{\mathbf{p}}_{\mathbf{p}_1,\mathbf{p}_2}|^2 f_{p12}\delta_{\mathbf{p}-\mathbf{p}_1-\mathbf{p}_2}\delta(\omega_{\mathbf{p}} - \omega_{\mathbf{p}_1} - \omega_{\mathbf{p}_2})d\mathbf{p}_{12} - 4\pi\int|V^{\mathbf{p}_1}_{\mathbf{p}_2,\mathbf{p}}|^2 f_{12p}\delta_{\mathbf{p}_1-\mathbf{p}_2-\mathbf{p}}\delta(\omega_{\mathbf{p}_1} - \omega_{\mathbf{p}_2} - \omega_{\mathbf{p}})d\mathbf{p}_{12} - 4\pi\int|V^{\mathbf{p}_2}_{\mathbf{p},\mathbf{p}_1}|^2 f_{2p1}\delta_{\mathbf{p}_2-\mathbf{p}-\mathbf{p}_1}\delta(\omega_{\mathbf{p}_2} - \omega_{\mathbf{p}} - \omega_{\mathbf{p}_1})d\mathbf{p}_{12},$$

$$\text{with}\quad f_{p12} = n_{\mathbf{p}_1} n_{\mathbf{p}_2} - n_{\mathbf{p}}(n_{\mathbf{p}_1} + n_{\mathbf{p}_2}). \tag{22}$$

We assume the wave vectors are signed variables and wave frequencies $\omega_{\mathbf{p}}$ are restricted to be positive. The magnitude of wave–wave interactions $J^{\mathbf{p}_2}_{\mathbf{p},\mathbf{p}_1}$ is a matrix representation of the coupling between triad members. It serves as a multiplier in the nonlinear convolution term in what is now commonly called the Zakharov equation, an equation in the Fourier space, for the wave field variable. This is also an expression that multiplies the cubic convolution term in the three-wave Hamiltonian.

We reiterate that typical assumptions needed for the derivation of kinetic equations are

- weak nonlinearity;
- Gaussian statistics of the interacting wave field in wavenumber space; and
- resonant wave–wave interactions.

[1] Note that we could have added the damping $\gamma_{\mathbf{p}}$ to the Hamiltonian equation of motion (10).

[2] We will revisit this assumption in section 5a.

We note that the derivation given here is schematic. A more systematic derivation can be obtained using only an assumption of weak nonlinearity.

c. The Boltzmann rate

The kinetic equation allows us to numerically estimate the lifetime of any given spectrum. In particular, we can define a wavenumber-dependent nonlinear time scale proportional to the inverse Boltzmann rate,

$$\tau_{\mathbf{p}}^{\mathrm{NL}} = \frac{n_{\mathbf{p}}}{\dot{n}_{\mathbf{p}}}. \tag{23}$$

This time scale characterizes the net rate at which the spectrum changes and can be directly calculated from the kinetic equation.

One can also define the characteristic linear time scale, equal to a wave period

$$\tau_{\mathbf{p}}^{\mathrm{L}} = 2\pi/\omega_{\mathbf{p}}.$$

The nondimensional ratio of these time scales can characterize the level of nonlinearity in the nonlinear system,

$$\epsilon_{\mathbf{p}} = \frac{\tau_{\mathbf{p}}^{\mathrm{L}}}{\tau_{\mathbf{p}}^{\mathrm{NL}}} = \frac{2\pi\dot{n}_{\mathbf{p}}}{n_{\mathbf{p}}\omega_{\mathbf{p}}}. \tag{24}$$

We refer to (24) as a normalized Boltzmann rate.

The normalized Boltzmann rate serves as a low-order consistency check for the various kinetic equation derivations. An $O(1)$ value of $\epsilon_{\mathbf{p}}$ implies that the derivation of the kinetic equation is internally inconsistent. The Boltzmann rate represents the net rate of transfer for wavenumber $\mathbf{p}$. The individual rates of transfer into and out of $\mathbf{p}$ (called Langevin rates) are typically greater than the Boltzmann rate (Müller et al. 1986; Pomphrey et al. 1980). This is particularly true in the induced diffusion regime (defined below in section 3) in which the rates of transfer into and out of $\mathbf{p}$ are one to three orders of magnitude larger than their residual and the Boltzmann rates we calculate are not appropriate for either spectral spikes or potentially for smooth, homogeneous but anisotropic spectra (Müller et al. 1986). Estimates of the individual rates of transfer into and out of $\mathbf{p}$ can be addressed through Langevin methods (Pomphrey et al. 1980). We focus here simply on the Boltzmann rate to demonstrate inconsistencies with the assumption of a slow time evolution. Estimates of the Boltzmann rate and $\epsilon_{\mathbf{p}}$ require integration of (22). In this manuscript, such integration is performed numerically.

3. Resonant wave–wave interactions: Nonrotational limit

How can one compare the function of two vectors $\mathbf{p}_1$ and $\mathbf{p}_2$ and their sum or difference? First one realizes that, out of six components of $\mathbf{p}_1$ and $\mathbf{p}_2$, only relative angles between wave vectors enter into the equation for matrix elements. That is because the matrix elements depend on the inner and outer products of wave vectors. The overall horizontal orientation of the wave vectors does not matter: relative angles can be determined from a triangle inequality and the magnitudes of the horizontal wave vectors $\mathbf{k}$, $\mathbf{k}_1$, and $\mathbf{k}_2$. Thus, the only needed components are $|\mathbf{k}|$, $|\mathbf{k}_1|$, $|\mathbf{k}_2|$, m, and m_1 (m_2 is computed from m and m_1). Further note that, in the $f = 0$ and hydrostatic limit, all matrix elements become scale-invariant functions. It is therefore sufficient to choose an arbitrary scalar value for $|\mathbf{k}|$ and m, because only $|\mathbf{k}_1|/|\mathbf{k}|$, $|\mathbf{k}_2|/|\mathbf{k}|$, and m_1/m enter the expressions for matrix elements. We make the particular (arbitrary) choice that $|\mathbf{k}| = m = 1$ for the purpose of numerical evaluation,[3] and thus the only independent variables to consider are $|\mathbf{k}_1|$, $|\mathbf{k}_2|$, and m_1. Finally, m_1 is determined from the resonance conditions, as explained in the next subsection below. As a result, we are left with a matrix element as a function of only two parameters, k_1 and k_2. This allows us to easily compare the values of matrix elements on the resonant manifold by plotting the values as a function of the two parameters.

a. Reduction to the resonant manifold

When confined to the traditional form of the kinetic equation, wave–wave interactions are constrained to the resonant manifolds defined by

$$\begin{cases} \mathbf{p} = \mathbf{p}_1 + \mathbf{p}_2 \\ \omega = \omega_1 + \omega_2 \end{cases}, \tag{25a}$$

$$\begin{cases} \mathbf{p}_1 = \mathbf{p}_2 + \mathbf{p} \\ \omega_1 = \omega_2 + \omega \end{cases}, \quad \text{and} \tag{25b}$$

$$\begin{cases} \mathbf{p}_2 = \mathbf{p} + \mathbf{p}_1 \\ \omega_2 = \omega + \omega_1 \end{cases}. \tag{25c}$$

To compare matrix elements on the resonant manifold, we are going to use the above resonant conditions and the internal wave dispersion relation (A4). To determine vertical components m_1 and m_2 of the interacting wave vectors, one has to solve the resulting quadratic equations. Without restricting generality, we choose $m > 0$. There are two solutions for m_1 and m_2 given below for each of the three resonance types described above.

[3] To derive the interaction matrix elements in the hydrostatic balance, we assumed that $k \ll m$. Once derivation is completed, values of k and m appear only as products, so it is consistent to make the choice $|\mathbf{k}| = m = 1$. This choice is made only in the present section.

Resonances of type (25a) give

$$\begin{cases} m_1 = \dfrac{m}{2|\mathbf{k}|}\left[|\mathbf{k}| + |\mathbf{k}_1| + |\mathbf{k}_2| + \sqrt{(|\mathbf{k}| + |\mathbf{k}_1| + |\mathbf{k}_2|)^2 - 4|\mathbf{k}||\mathbf{k}_1|}\right] \\ m_2 = m - m_1 \end{cases} \text{ and} \tag{26a}$$

$$\begin{cases} m_1 = \dfrac{m}{2|\mathbf{k}|}\left(|\mathbf{k}| + |\mathbf{k}_1| + |\mathbf{k}_2| + \sqrt{(|\mathbf{k}| + |\mathbf{k}_1| + |\mathbf{k}_2|)^2 - 4|\mathbf{k}||\mathbf{k}_1|}\right) \\ m_2 = m - m_1 \end{cases}. \tag{26b}$$

Note that, because of the symmetry, (26a) translates to (26b) if wavenumbers 1 and 2 are exchanged.

Resonances of type (25b) give

$$\begin{cases} m_2 = \dfrac{m}{2|\mathbf{k}|}\left[|\mathbf{k}| - |\mathbf{k}_1| - |\mathbf{k}_2| + \sqrt{(|\mathbf{k}| - |\mathbf{k}_1| - |\mathbf{k}_2|)^2 + 4|\mathbf{k}||\mathbf{k}_2|}\right] \\ m_1 = m + m_2 \end{cases} \text{ and} \tag{27a}$$

$$\begin{cases} m_2 = \dfrac{m}{2|\mathbf{k}|}\left[|\mathbf{k}| + |\mathbf{k}_1| - |\mathbf{k}_2| + \sqrt{(|\mathbf{k}| + |\mathbf{k}_1| - |\mathbf{k}_2|)^2 + 4|\mathbf{k}||\mathbf{k}_2|}\right] \\ m_1 = m + m_2 \end{cases}. \tag{27b}$$

Resonances of type (25c) give

$$\begin{cases} m_1 = \dfrac{m}{2|\mathbf{k}|}\left[|\mathbf{k}| - |\mathbf{k}_1| - |\mathbf{k}_2| + \sqrt{(|\mathbf{k}| - |\mathbf{k}_1| - |\mathbf{k}_2|)^2 + 4|\mathbf{k}||\mathbf{k}_1|}\right] \\ m_2 = m + m_1. \end{cases} \text{ and} \tag{28a}$$

$$\begin{cases} m_1 = \dfrac{m}{2|\mathbf{k}|}\left(|\mathbf{k}| - |\mathbf{k}_1| + |\mathbf{k}_2| + \sqrt{(|\mathbf{k}| - |\mathbf{k}_1| + |\mathbf{k}_2|)^2 + 4|\mathbf{k}||\mathbf{k}_1|}\right) \\ m_2 = m + m_1 \end{cases}. \tag{28b}$$

Because of the symmetries of the problem, (27a) is equivalent to (28a) and (27b) is equivalent to (28b) if wavenumbers 1 and 2 are exchanged.

b. Comparison of matrix elements

As explained above, we assume $f = 0$ and hydrostatic balance. Such a choice makes the matrix element scale-invariant functions that depend only upon $|\mathbf{k}_1|$ and $|\mathbf{k}_2|$. As a consequence of the triangle inequality, we need to consider matrix elements only within a "kinematic box" defined by

$$||\mathbf{k}_1| - |\mathbf{k}_2|| < |\mathbf{k}| < |\mathbf{k}_1| + |\mathbf{k}_2|.$$

The matrix elements will have different values depending on the dimensions so that isopycnal and Eulerian approaches will give different values (A2) and (A3). To address this issue in the simplest possible way, we multiply each matrix element by a dimensional number chosen so that all matrix elements are equivalent for some specific wave vector. In particular, we choose the scaling constant so that $|V(|\mathbf{k}_1| = 1, |\mathbf{k}_2| = 1)|^2 = 1$. This allows a transparent comparison without worrying about dimensional differences between various formulations.

1) RESONANCES OF THE SUM TYPE [(25A)]

Figure 1 presents the values of the matrix element $|V^{\mathbf{p}}_{\mathbf{p}_1,\mathbf{p}_2(26b)}|^2$ on the resonant submanifold given explicitly by (26b). All approaches give equivalent results. This is confirmed by plotting the relative ratio between these approaches, and it is given by numerical noise (not

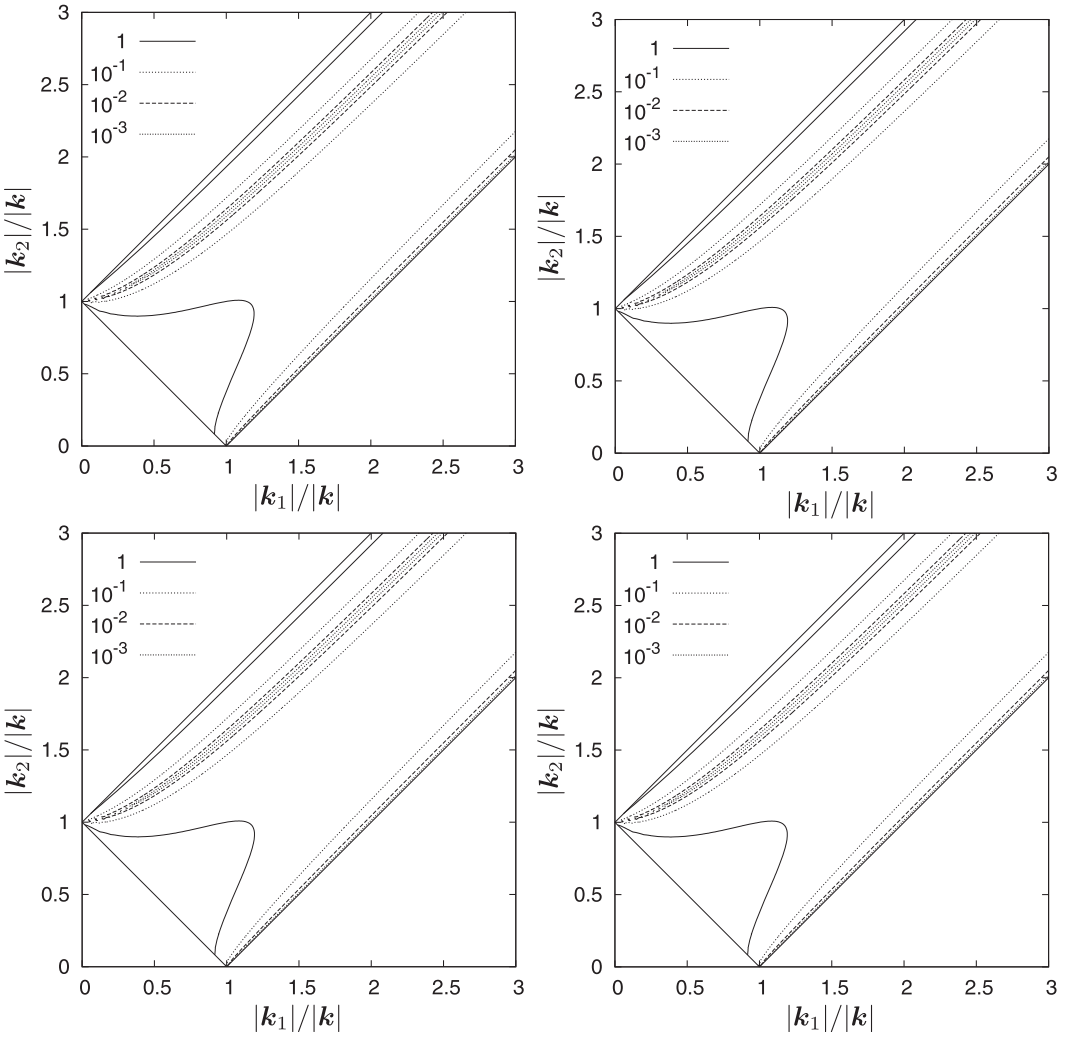

FIG. 1. Contours of matrix elements $|V^{\mathbf{p}}_{\mathbf{p}_1,\mathbf{p}_2(26b)}|^2$ given by the solution (29): (top left) $|V^{\mathbf{p}\ \mathrm{MO}}_{\mathbf{p}_1,\mathbf{p}_2(26b)}|^2$ according to Müller and Olbers (1975); (top right) $|V^{\mathbf{p}\ \mathrm{V}}_{\mathbf{p}_1,\mathbf{p}_2(26b)}|^2$ according to Voronovich (1979); (bottom left) $|V^{\mathbf{p}\ \mathrm{CZ}}_{\mathbf{p}_1,\mathbf{p}_2(26b)}|^2$ according to Caillol and Zeitlin (2000); and (bottom right) $|V^{\mathbf{p}\ \mathrm{H}}_{\mathbf{p}_1,\mathbf{p}_2(26b)}|^2$ according to Lvov and Tabak (2001).

shown). The solution in (26a) gives the same matrix elements but with $|\mathbf{k}_1|$ and $|\mathbf{k}_2|$ exchanged because of their symmetries.

2) Resonances of the difference type [(25b) and (25c)]

We then turn our attention to resonances of difference type (25b) for which (25c) could be obtained by symmetrical exchange of the indices. All the matrix elements $|V^{\mathbf{p}_1}_{\mathbf{p}_2,\mathbf{p}(27a)}|^2$ on the resonant submanifold (27a) are shown in Fig. 2. All the matrix elements are equivalent. The relative differences between different approaches are given by numerical noise (not shown). Finally, $|V^{\mathbf{p}_1}_{\mathbf{p}_2,\mathbf{p}(27b)}|^2$ on the resonant submanifold (27b) is shown in Fig. 3. Again, all the matrix elements are equivalent. The solutions (28a) and (28b) give the same matrix elements but with $|\mathbf{k}_1|$ and $|\mathbf{k}_2|$ exchanged as the solutions (27a) and (27b) because of their symmetries.

3) Special triads

Three simple interaction mechanisms are identified by McComas and Bretherton (1977) in the limit of an extreme scale separation. In this subsection, we look in closer detail at these special limiting triads to confirm that all matrix elements are indeed asymptotically consistent. The limiting cases are as follows:

- The vertical backscattering of a high-frequency wave by a low-frequency wave of twice the vertical wavenumber into a second high-frequency wave of oppositely signed

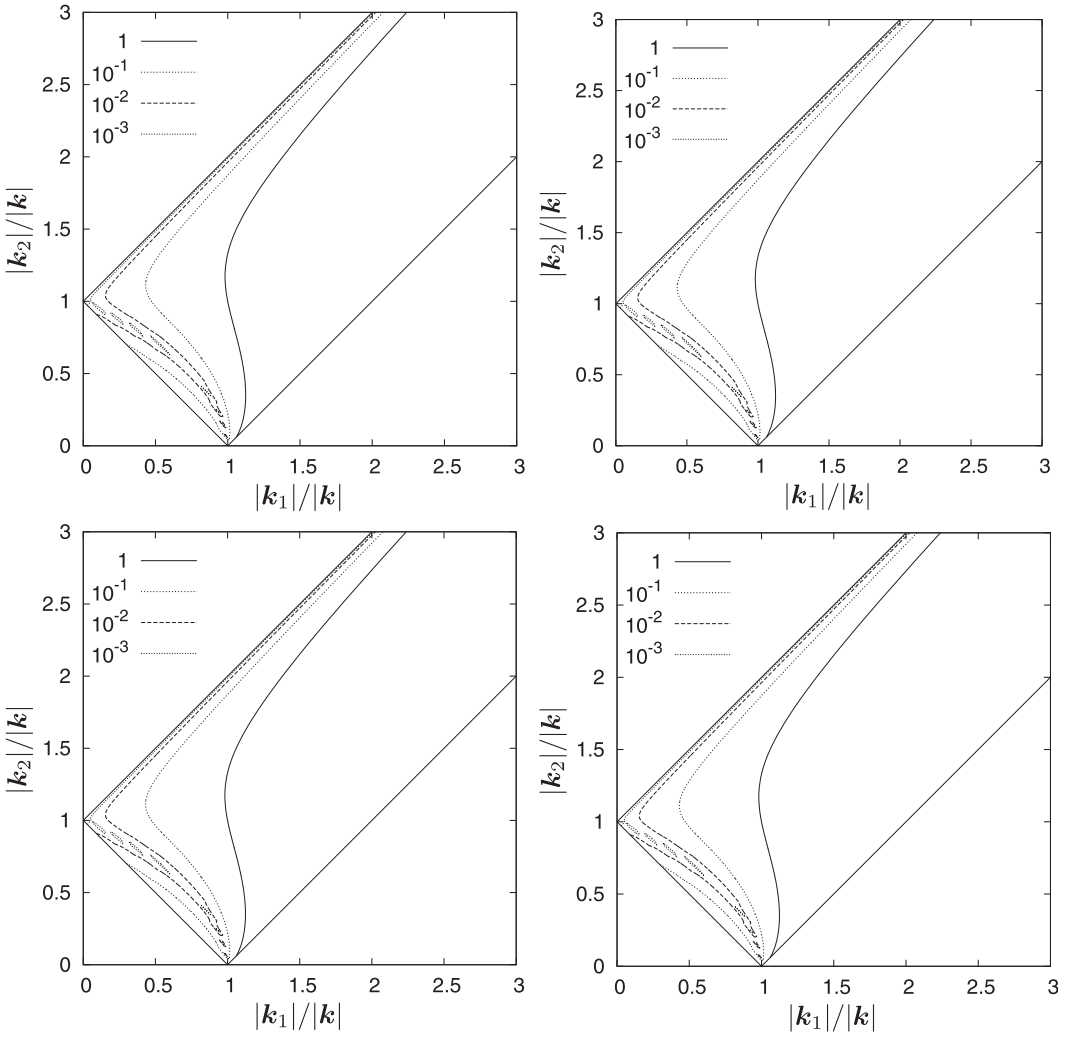

FIG. 2. Contour lines of values of matrix elements $|V^{\mathbf{p}_1}_{\mathbf{p}_2,\mathbf{p}(27a)}|^2$ given by the solution (27a): (top left) $|V^{\mathbf{p}_1\ \mathrm{MO}}_{\mathbf{p}_2,\mathbf{p}(27a)}|^2$ according to Müller and Olbers (1975); (top right) $|V^{\mathbf{p}_1\ \mathrm{V}}_{\mathbf{p}_2,\mathbf{p}(27a)}|^2$ according to Voronovich (1979); (bottom left) $|V^{\mathbf{p}_1\ \mathrm{CZ}}_{\mathbf{p}_2,\mathbf{p}(27a)}|^2$ according to Caillol and Zeitlin (2000); and (bottom right) $|V^{\mathbf{p}_1\ \mathrm{H}}_{\mathbf{p}_2,\mathbf{p}(27a)}|^2$ according to Lvov and Tabak (2001).

vertical wavenumber and nearly the same wavenumber magnitude. This type of scattering is called elastic scattering. The solution (26a) in the limit $|\mathbf{k}_1| \to 0$ corresponds to this type of special triad.

- The scattering of a high-frequency wave by a low-frequency, small-wavenumber wave into a second, nearly identical, high-frequency large-wavenumber wave. This type of scattering is called induced diffusion. The solution (26b) in the limit that $|\mathbf{k}_1| \to 0$ corresponds to this type of special triad.
- The decay of a low-wavenumber wave into two high vertical wavenumber waves of approximately one-half the frequency. This is called parametric subharmonic instability (PSI). The solution (27a) in the limit that $|\mathbf{k}_1| \to 0$ corresponds to this type of triad.

To study the behavior of the matrix elements in the special triad cases, we need to construct a triad that belongs to one of the special cases. There are many ways one can do that; that is, there are many ways to parameterize $(|\mathbf{k}_1|, |\mathbf{k}_2|)$ in such a way that they span a special triad case. We choose one such particular parameterization; that is, we choose

$$(|\mathbf{k}_1|, |\mathbf{k}_2|) = (\epsilon, \epsilon/3 + 1)|\mathbf{k}|.$$

This line is defined in such a way so that it originates from the corner of the kinematic box in Figs. 1–3 at $(|\mathbf{k}_1|, |\mathbf{k}_2|) = (0, |\mathbf{k}|)$ and has a slope of 1/3. The slope of this line is arbitrary. We could have taken $\epsilon/4$ or $\epsilon/2$. The matrix elements here are shown as functions of ϵ in Fig. 4.

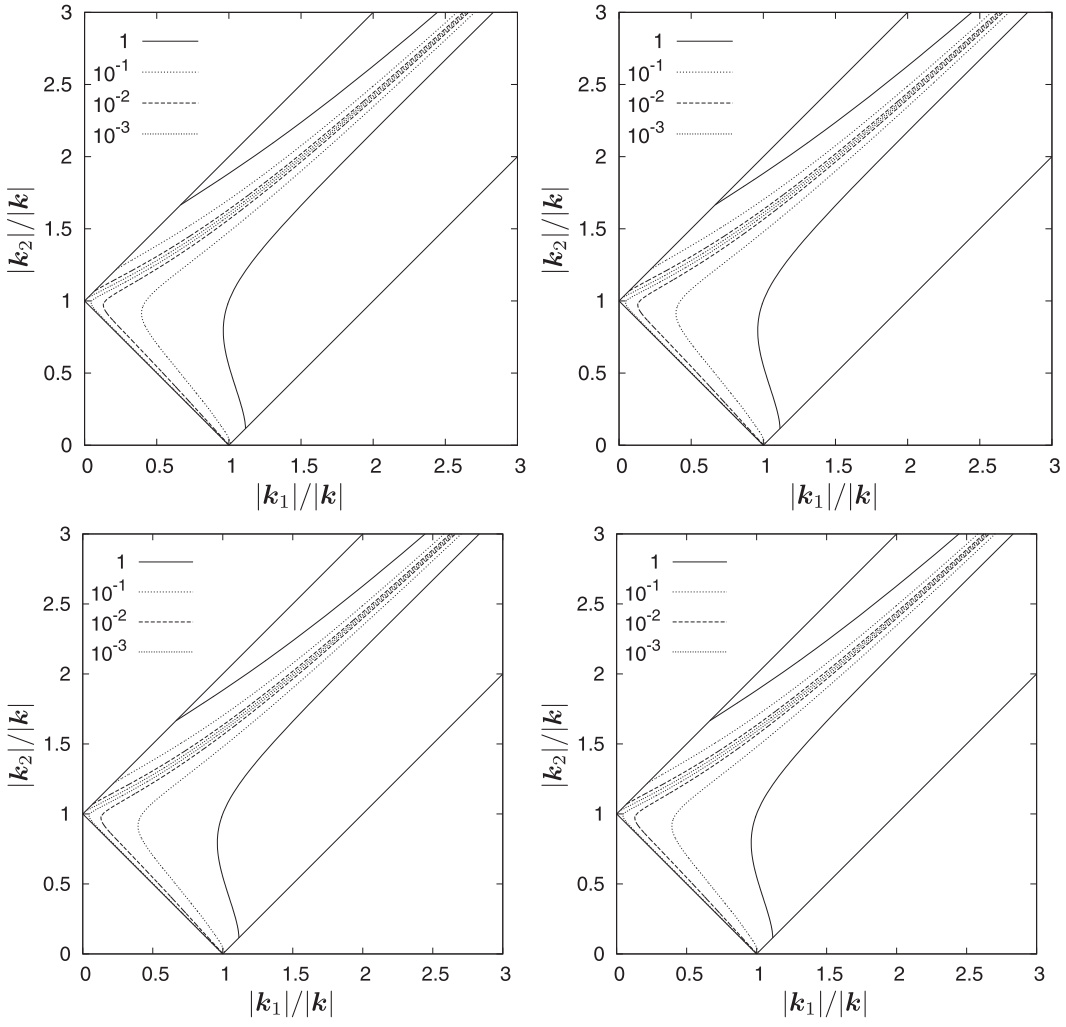

FIG. 3. Contour lines of values of matrix $|V^{\mathbf{p}_1}_{\mathbf{p}_2,\mathbf{p}(27b)}|^2$ given by the solution (27b): (top left) $|V^{\mathbf{p}_1\ \mathrm{MO}}_{\mathbf{p}_2,\mathbf{p}(27b)}|^2$ according to Müller and Olbers (1975); (top right) $|V^{\mathbf{p}_1\ \mathrm{V}}_{\mathbf{p}_2,\mathbf{p}(27b)}|^2$ according to Voronovich (1979); (bottom left) $|V^{\mathbf{p}_1\ \mathrm{CZ}}_{\mathbf{p}_2,\mathbf{p}(27b)}|^2$ according to Caillol and Zeitlin (2000); and (bottom right) $|V^{\mathbf{p}_1\ \mathrm{H}}_{\mathbf{p}_2,\mathbf{p}(27b)}|^2$ according to Lvov and Tabak (2001).

We see that all four approaches are again equivalent on the resonant manifold for the case of special triads.

In this section, we demonstrated that all four approaches we considered produce equivalent results on the resonant manifold in the absence of background rotation. This statement is not trivial, given the different assumptions and coordinate systems that have been used for the various kinetic equation derivations.

4. Resonant wave–wave interactions: In the presence of background rotations

In the presence of background rotation, the matrix elements lose their scale invariance because of the introduction of an additional time scale $(1/f)$ in the system. Consequently, the comparison of matrix elements is performed as a function of four independent parameters.

We perform this comparison in the frequency–vertical wavenumber domain. In particular, for arbitrary ω, ω_1, m, and m_1, ω_2, and m_2 can be calculated by requiring that they satisfy the resonant conditions $\omega = \omega_1 + \omega_2$ and $m = m_1 + m_2$. We then can check whether the corresponding horizontal wavenumber magnitudes k, given by

$$k_i = \frac{m_i N \rho_o}{g}\sqrt{\omega_i^2 - f^2} \text{ (isopycnal coordinates)} \quad \text{and}$$

$$k_i = m_i \frac{\sqrt{\omega_i^2 - f^2}}{N} \text{ (Lagrangian coordinates)} \qquad (29)$$

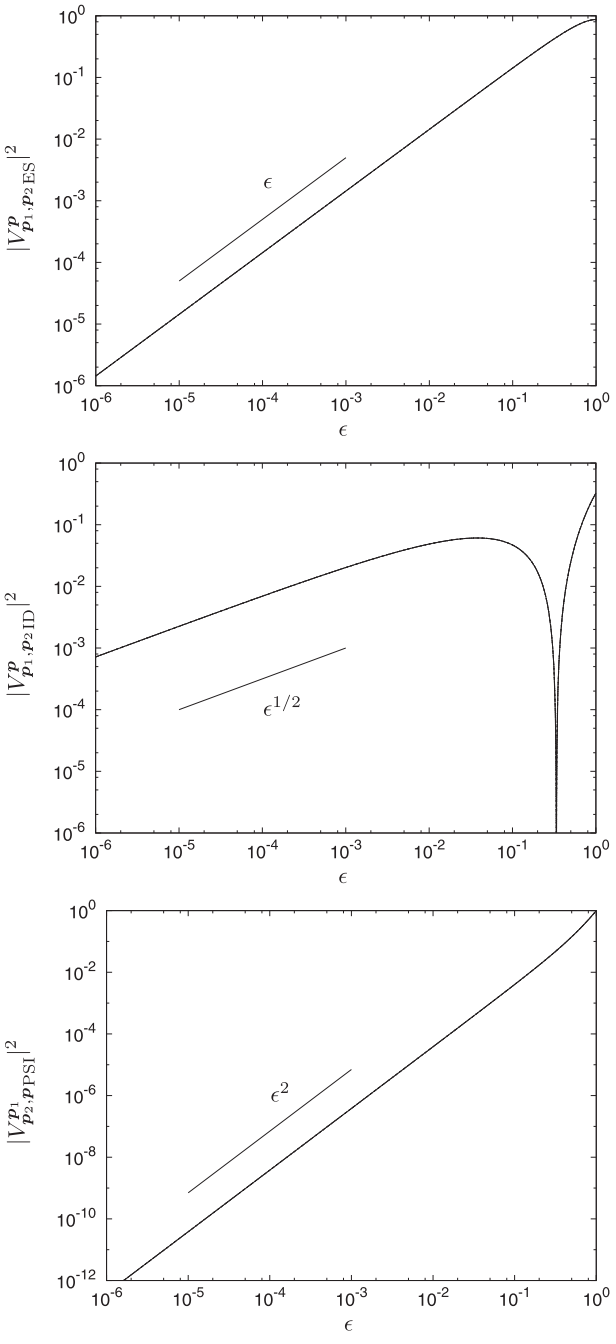

FIG. 4. (top) Matrix elements $|V^{\mathbf{p}}_{\mathbf{p}_1,\mathbf{p}_2\mathrm{ES}}|^2$ given by the solution (26a). (middle) Matrix elements $|V^{\mathbf{p}}_{\mathbf{p}_1,\mathbf{p}_2\mathrm{ID}}|^2$ given by the solution (26b). (bottom) Matrix elements $|V^{\mathbf{p}}_{\mathbf{p}_1,\mathbf{p}\mathrm{PSI}}|^2$ given by the solution (27a), which gives PSI as $|\mathbf{k}_1| \to 0$ ($\epsilon \to 0$). The matrix elements here are shown as functions of ε such that $(|\mathbf{k}_1|, |\mathbf{k}_2|) = (\epsilon, \epsilon/3 + 1)|\mathbf{k}|$. All four versions of the matrix elements are plotted here: the appearance of a single line in each panel testifies to the similarity of the elements on the resonant manifold.

satisfy the triangle inequality. The matrix elements of the isopycnal and Lagrangian coordinate representations are then calculated. We have performed this comparison for 10^{12} points on the resonant manifold. After being multiplied by an appropriate dimensional number to convert between Eulerian and isopycnal coordinate systems, the two matrix elements coincide up to machine precision.

One might, with sufficient experience, regard this as an intuitive statement. It is, however, far from trivial given the different assumptions and coordinate representations. In particular, we note that derivations of the wave amplitude evolution equation in Lagrangian coordinates (Olbers 1976; McComas 1975; Meiss et al. 1979) do not explicitly contain a potential vorticity conservation statement corresponding to assumption (4) in the isopycnal coordinate (Lvov and Tabak 2004) derivation. We have inferred that the Lagrangian coordinate derivation conserves potential vorticity as that system is projected upon the linear modes of the system having zero perturbation potential vorticity.

5. Resonance broadening and numerical methods

a. *Nonlinear frequency renormalization as a result of nonlinear wave–wave interactions*

The resonant interaction approximation is a self-consistent mathematical simplification, which reduces the complexity of the problem for weakly nonlinear systems. As nonlinearity increases, near-resonant interactions become more and more pronounced and need to be addressed. Moreover, near-resonant interactions play a major role in numerical simulations on a discrete grid (Lvov et al. 2006), for time evolution of discrete systems (Gershgorin et al. 2007), in acoustic turbulence (Lvov et al. 1997), surface gravity waves (Janssen 2003; Yuen and Lake 1982), and internal waves (Voronovich et al. 2006; Annenkov and Shrira 2006).

To take into account the effects of near-resonant interactions self-consistently, we revisit section 2b. Now we do not take the limit $\tilde{\Gamma}_{\mathbf{p}\mathbf{p}_1\mathbf{p}_2} \to 0$ in Eq. (19). Then, instead of the kinetic equation with the frequency-conserving delta function, we obtain the generalized kinetic equation

$$\frac{dn_{\mathbf{p}}}{dt} = 4\int |V^{\mathbf{p}}_{\mathbf{p}_1,\mathbf{p}_2}|^2 f_{p12}\delta_{\mathbf{p}-\mathbf{p}_1-\mathbf{p}_2}\mathcal{L}(\omega_{\mathbf{p}} - \omega_{\mathbf{p}_1} - \omega_{\mathbf{p}_2})d\mathbf{p}_{12}$$
$$- 4\int |V^{\mathbf{p}_1}_{\mathbf{p}_2,\mathbf{p}}|^2 f_{12p}\delta_{\mathbf{p}_1-\mathbf{p}_2-\mathbf{p}}\mathcal{L}(\omega_{\mathbf{p}_1} - \omega_{\mathbf{p}_2} - \omega_{\mathbf{p}})d\mathbf{p}_{12}$$
$$- 4\int |V^{\mathbf{p}_2}_{\mathbf{p},\mathbf{p}_1}|^2 f_{2p1}\delta_{\mathbf{p}_2-\mathbf{p}-\mathbf{p}_1}\mathcal{L}(\omega_{\mathbf{p}_2} - \omega_{\mathbf{p}} - \omega_{\mathbf{p}_1})d\mathbf{p}_{12},$$
$$\text{with} \quad f_{p12} = n_{\mathbf{p}_1}n_{\mathbf{p}_2} - n_{\mathbf{p}}(n_{\mathbf{p}_1} + n_{\mathbf{p}_2}), \tag{30}$$

where $\mathcal{L}$ is defined as

$$\mathcal{L}(\Delta\omega) = \frac{\Gamma_{k12}}{(\Delta\omega)^2 + \Gamma_{k12}^2}. \tag{31}$$

Here, Γ_{k12} is the total broadening of each particular resonance and is given below in (32) and (33).

The difference between kinetic equation (22) and the generalized kinetic equation (30) is that the energy-conserving delta functions in (22), $\delta(\omega_{\mathbf{p}} - \omega_{\mathbf{p}_1} - \omega_{\mathbf{p}_2})$, was "broadened." The physical motivation for this broadening is the following: When the resonant kinetic equation is derived, it is assumed that the amplitude of each plane wave is constant in time or, in other words, that the lifetime of single plane wave is infinite. The resulting kinetic equation nevertheless predicts that wave amplitude changes. Consequently, the wave lifetime is finite. For a small level of nonlinearity, this distinction is not significant, and resonant kinetic equation constitutes a self-consistent description. For larger values of nonlinearity, this is no longer the case, and the wave lifetime is finite and amplitude changes need to be taken into account. Consequently, interactions may not be strictly resonant. This statement also follows from the Fourier uncertainty principle. Waves with varying amplitude cannot be represented by a single Fourier component. This effect is larger for larger normalized Boltzmann rates.

If the nonlinear frequency renormalization tends to zero (i.e., $\Gamma_{k12} \to 0$), $\mathcal{L}$ reduces to the delta function [compare to (21)],

$$\lim_{\Gamma_{k12}\to 0} \mathcal{L}(\Delta\omega) = \pi\delta(\Delta\omega).$$

Consequently, in the limit resonant interactions (i.e., no broadening), (30) reduces to (22).

If, on the other hand, one does not take the $\tilde{\Gamma}_{\mathbf{p}\mathbf{p}_1\mathbf{p}_2} \to 0$ limit, then one has to calculate $\Gamma_{\mathbf{p}\mathbf{p}_1\mathbf{p}_2}$ self-consistently. To achieve this, we realize that by deriving the generalized kinetic Eq. (30) we allow changes in wave amplitude. The rate of change can be identified from Eq. (30) in the following way: Let us go through (30) term by term and identify all terms that multiply the $n_{\mathbf{p}}$ on the right-hand side. Those terms can be loosely interpreted as a nonlinear wave damping acting on the given wavenumber,

$$\begin{aligned}\gamma_{\mathbf{p}} = {} & 4\int |V^{\mathbf{p}}_{\mathbf{p}_1,\mathbf{p}_2}|^2 (n_{\mathbf{p}_1} + n_{\mathbf{p}_2})\delta_{\mathbf{p}-\mathbf{p}_1-\mathbf{p}_2}\mathcal{L}(\omega_{\mathbf{p}} - \omega_{\mathbf{p}_1} - \omega_{\mathbf{p}_2})d\mathbf{p}_{12} \\ & - 4\int |V^{\mathbf{p}_1}_{\mathbf{p}_2,\mathbf{p}}|^2 (n_{\mathbf{p}_2} - n_{\mathbf{p}_1})\delta_{\mathbf{p}_1-\mathbf{p}_2-\mathbf{p}}\mathcal{L}(\omega_{\mathbf{p}_1} - \omega_{\mathbf{p}_2} - \omega_{\mathbf{p}})d\mathbf{p}_{12} \\ & - 4\int |V^{\mathbf{p}_2}_{\mathbf{p},\mathbf{p}_1}|^2 (n_{\mathbf{p}_1} - n_{\mathbf{p}_2})\delta_{\mathbf{p}_2-\mathbf{p}-\mathbf{p}_1}\mathcal{L}(\omega_{\mathbf{p}_2} - \omega_{\mathbf{p}} - \omega_{\mathbf{p}_1})d\mathbf{p}_{12}.\end{aligned} \tag{32}$$

The interpretation of this formula is the following: Nonlinear wave–wave interactions lead to the change of wave amplitude, which in turn makes the lifetime of the waves to be finite. This, in turn, makes the interactions to be near resonant.

Replacement of $\tilde{\gamma}_{\mathbf{p}}$ in (18) by $\gamma_{\mathbf{p}}$ in (32) corresponds to the renormalization or dressing of bare dumping by the nonlinear dumping that appears as a result of wave–wave interactions. This methodology is well studied in the context of diagrammatic technique (Lvov et al. 1997). Consequently, the $\tilde{\Gamma}_{\mathbf{p}_1\mathbf{p}_2\mathbf{p}_3}$ in (19) defined in (20) gets renormalized to

$$\Gamma_{k12} = \gamma_{\mathbf{p}} + \gamma_{\mathbf{p}_1} + \gamma_{\mathbf{p}_2}. \tag{33}$$

It means that the total resonance broadening is the sum of total broadenings of all individual frequency broadening and can be thus seen as the "triad interaction" frequency. We also note that dumping is intrinsically related to broadening, just as in the case of simple harmonic oscillator.

A rigorous derivation of the kinetic Eq. (30) with a broadened delta function (31)–(33) is given in detail for a generic three-wave Hamiltonian system in Lvov et al. (1997). The derivation is based upon the Wyld diagrammatic technique for nonequilibrium wave systems and utilizes the Dyson–Wyld line resummation. This resummation permits an analytical resummation of the infinite series of reducible diagrams for Greens functions and double correlators. We emphasize however that the approach is perturbative in nature and that there are neglected parts of the infinite diagrammatic series.

A self-consistent estimate of $\gamma_{\mathbf{p}}$ requires an iterative solution of (30) and (32) over the entire field: The width of the resonance (32) depends on the lifetime of an individual wave [from (30)], which in turn depends on the width of the resonance (33). This numerically intensive computation is beyond the scope of this manuscript. Instead, we make the uncontrolled approximation that

$$\gamma_{\mathbf{p}} = C\omega_{\mathbf{p}}, \tag{34}$$

where C is the dimensionless constant that defines how strongly a particular frequency gets broadened by nonlinear wave–wave interactions.

We note the choice (34) is made for illustration purposes only, we certainly do not claim it to be self consistent. Below, we will take C to be 10^{-3}, 10^{-2}, and 10^{-1}. These values are rather small; therefore, we remain in the closest proximity to the resonant interactions. To show the effect of strong resonant manifold smearing, we also investigate the case with $C = 0.5$.

We note in passing that the near-resonant interactions of the waves were also considered in Janssen (2003). There, instead of our $\mathcal{L}(x)$ function, given by (31), the corresponding function was given by $\sin(\pi x)/x$. We have shown in Kramer et al. (2003) that the resulting kinetic equation does not retain positive definite values of wave action. To get around that difficulty, self-consistent formulas for broadening should be used. Here we discuss such formulas, which are based upon a rigorous diagrammatic resummation.

b. Numerical methods

Estimates of near-resonant transfers are obtained by assuming horizontal isotropy and integrating (30) over horizontal azimuth,

$$\begin{aligned}\frac{\partial n_{\mathbf{p}}}{\partial t} &= 4\pi \int \frac{k_1 k_2}{S_{p12}} |V^{\mathbf{p}}_{\mathbf{p}_1,\mathbf{p}_2}|^2 f_{p12} \delta_{\mathbf{p}-\mathbf{p}_1-\mathbf{p}_2} \mathcal{L}(\omega_{\mathbf{p}} - \omega_{\mathbf{p}_1} - \omega_{\mathbf{p}_2})\, dk_1\, dk_2\, dm_1 \\ &- 4\pi \int \frac{k_1 k_2}{S_{12p}} |V^{\mathbf{p}_1}_{\mathbf{p}_2,\mathbf{p}}|^2 f_{12p} \delta_{\mathbf{p}_1-\mathbf{p}_2-\mathbf{p}} \mathcal{L}(\omega_{\mathbf{p}_1} - \omega_{\mathbf{p}_2} - \omega_{\mathbf{p}})\, dk_1\, dk_2\, dm_1 \\ &- 4\pi \int \frac{k_1 k_2}{S_{2p1}} |V^{\mathbf{p}_2}_{\mathbf{p},\mathbf{p}_1}|^2 f_{2p1} \delta_{\mathbf{p}_2-\mathbf{p}-\mathbf{p}_1} \mathcal{L}(\omega_{\mathbf{p}_2} - \omega_{\mathbf{p}} - \omega_{\mathbf{p}_1})\, dk_1\, dk_2\, dm_1, \end{aligned} \tag{35}$$

where S_{p12} is the area of the triangle $\mathbf{k} = \mathbf{k}_1 + \mathbf{k}_2$. We numerically integrated (35) for $\mathbf{p}$ that have frequencies from f to N and vertical wavenumbers from $2\pi/(2b)$ to $260\pi/(2b)$. The limits of integration are restricted by horizontal wavenumbers from $2\pi/10^5$ to $2\pi/5$ m^{-1}, vertical wavenumbers from $2\pi/(2b)$ to $2\pi/5$ m^{-1}, and frequencies from f to N. The integrals over k_1 and k_2 are obtained in the kinematic box in k_1–k_2 space. The grids in the k_1–k_2 domain have 2^{17} points that are distributed heavily around the corner of the kinematic box. The integral over m_1 is obtained with 2^{13} grid points, which are also distributed heavily for the small vertical wavenumbers whose absolute values are less than $5m$, where m is the vertical wavenumber.

To estimate the normalized Boltzmann rate, we need to choose a form of spectral energy density of internal waves. We utilize the Garrett and Munk spectrum as commonly used representation of the internal waves,

$$E(\omega, m) = \frac{4f}{\pi^2 m_*} E_0 \frac{1}{1 + \left(\dfrac{m}{m_*}\right)^2} \frac{1}{\omega\sqrt{\omega^2 - f^2}}. \tag{36}$$

Here, the reference wavenumber is given by

$$m_* = \pi j_*/b, \tag{37}$$

in which the variable j represents the vertical mode number of an ocean with an exponential buoyancy frequency profile having a thermocline scale height of $b = 1300$ m.

We choose the following set of parameters:

- $b = 1300$ m in the GM model;
- the total energy is set as

$$E_0 = 30 \times 10^{-4}\ \mathrm{m^2\ s^{-2}};$$

  inertial frequency is given by $f = 10^{-4}$ rad s^{-1}, and buoyancy frequency is given by $N_0 = 5 \times 10^{-3}$ rad s^{-1};
- the reference density is taken to be $\rho_0 = 10^3$ kg m^{-3}; and
- a rolloff wavenumber $m_* = N/N_o \pi j_*/b$ equivalent to mode 3, $j_* = 3$.

We then calculate the normalized Boltzmann rate (24) using four values of C in (34): $C = 10^{-3}$, $C = 10^{-2}$, $C = 10^{-1}$, and $C = 0.5$.

Our simulations do show some sensitivity to the spectral boundaries and show significant sensitivity for the choice of $\gamma_{\mathbf{p}}$, especially for relatively large values of $\gamma_{\mathbf{p}}$. Sorting out these sensitivities and finding a self-consistent value of $\gamma_{\mathbf{p}}$ is the subject of current research.

6. Time scales

a. Resonant interactions

Here, we present evaluations of the kinetic equation (35) with a broadened delta function (31) and (34). These estimates differ from evaluations presented in Olbers

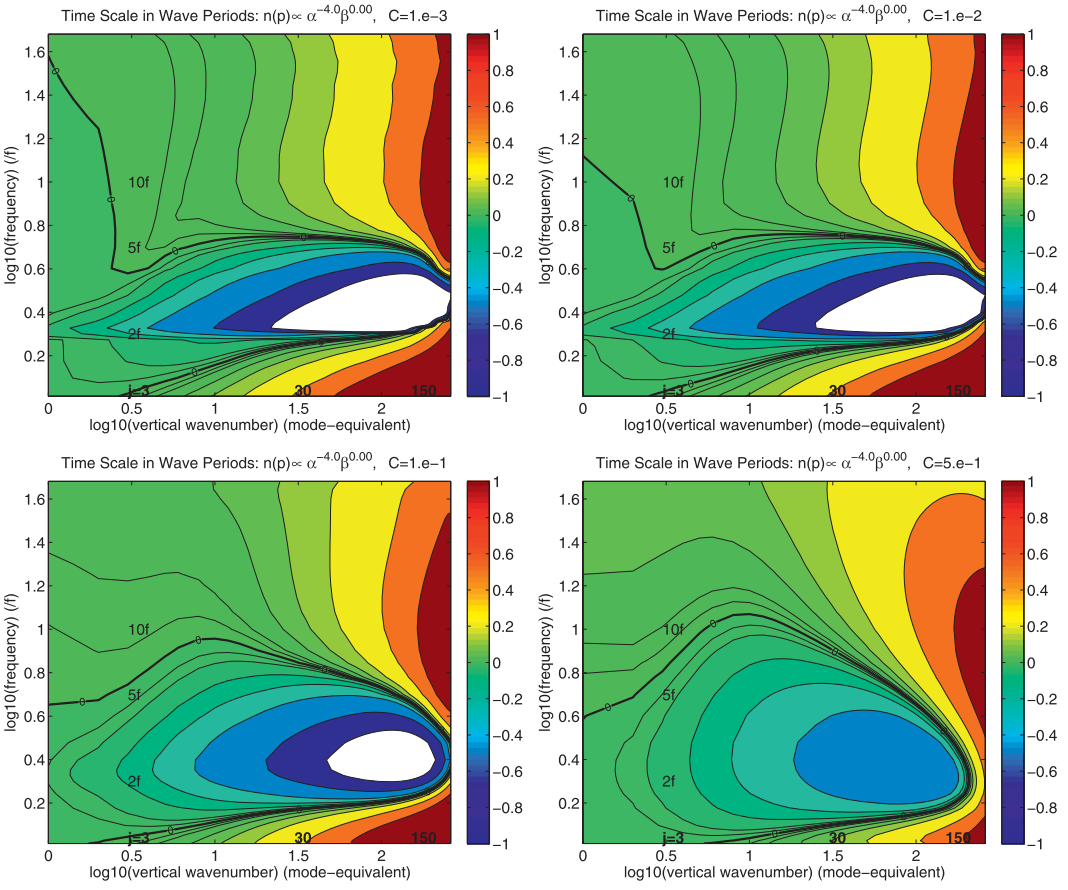

FIG. 5. Normalized Boltzmann rates (24) for the Garrett and Munk spectrum (36) calculated via (30). Figures represent normalized Boltzmann rate calculated using Lvov and Tabak (2004), Eq. (A21) with (top left) $C = 10^{-3}$, (top right) $C = 10^{-2}$, (bottom left) $C = 10^{-1}$, and (bottom right) $C = 0.5$. The white region corresponds to extremely fast time scales, faster than a linear time scale. The horizontal axis is vertical wavenumber expressed as the equivalent mode number of a buoyancy-scaled basin 1300 m deep.

(1976), McComas (1977), McComas and Müller (1981a), and Pomphrey et al. (1980) in that the numerical algorithm includes a finite breadth to the resonance surface, whereas previous evaluations have been exactly resonant. Results discussed in this section are as close to resonant as we can make ($C = 1 \times 10^{-3}$).

Results are presented in Fig. 5 for different values of C. We see that for small vertical wavenumbers the normalized Boltzmann rate is of the order of a tenth of the wave period. This can be argued to be relatively within the domain of weak nonlinearity. However, for increased wavenumbers the level of nonlinearity increases and reaches the level of wave period (red or dark blue). There is also a white region indicating values smaller than minus one.

We also define a "zero curve": It is the locus of wavenumber–frequency where the normalized Boltzmann rate and time derivative of wave action is exactly zero. The zero curve clearly delineates a pattern of energy gain for frequencies $f < \omega < 2f$, energy loss for frequencies $2f < \omega < 5f$, and energy gain for frequencies $5f < \omega < N_0$. We interpret the relatively sharp boundary between energy gain and energy loss across $\omega = 2f$ as being related to the parametric subharmonic instability and the transition from energy loss to energy gain at $\omega = 5f$ as a transition from energy loss associated with the parametric subharmonic instability to energy gain associated with the elastic scattering mechanism. See section 7 for further details about this high-frequency interpretation.

The $O(1)$ normalized Boltzmann rates at high vertical wavenumber are surprising given the substantial literature that regards the GM spectrum as a stationary state. We do not believe this to be an artifact of the numerical scheme for the following reasons: First, numerical evaluations of the integrand conserve energy to within numerical precision as the resonance surface is approached, consistent with energy conservation property associated with the frequency delta function. Second, the time scales

TABLE 2. Numerical evaluations of $\int_f^N E(m,\omega)d\omega$ for vertical mode numbers 1–8. The sum is given in the rightmost column.

$\dot{E}\times10^{-10}$ W kg^{-1}	Mode	1	2	3	4	5	6	7	8	Σ
Lvov and Tabak (2004)	GM76	−1.46	−1.72	−1.76	−1.69	−1.57	−1.40	−1.08	−0.81	−11.5
Pomphrey et al. (1980)	GM76	−1.83	−2.17	−2.17	−1.83	−1.67	−1.00			−10.7

converge as the resonant width is reduced, as demonstrated by the minimal difference in time scales using $C = 1\times10^{-3}$ and 1×10^{-2}. Third, our results are consistent with approximate analytic expressions (e.g., McComas and Müller 1981b) for the Boltzmann rate. Finally, in view of the differences in the representation of the wave field, numerical codes, and display of results, we interpret our resonant ($C = 0.001$) results as being consistent with numerical evaluations of the resonant kinetic equations presented in Olbers (1976), McComas (1977), McComas and Müller (1981a), and Pomphrey et al. (1980).

As a quantitative example, consider estimates of the time rate of change of low-mode energy appearing in Table 1 of Pomphrey et al. (1980), which is repeated as row 3 of our Table 2[4]. We find agreement to better than a factor of 2. To explain the remaining differences, one has to examine the details: Pomphrey et al. (1980) use a Coriolis frequency corresponding to 30° latitude; neglect internal waves having horizontal wavelengths greater than 100 km (same as here); and exclude frequencies $\omega > N_o/3$, with $N_o = 3$ cph. We include frequencies $f < \omega < N_o$ with Coriolis frequency corresponding to 45° latitude. Of possible significance is that Pomphrey et al. (1980) use a vertical mode decomposition with exponential stratification with scale height $b = 1200$ m (we use constant N and assume an ocean depth equivalent to $b = 1300$ m). Table 2 presents estimates of the energy transfer rate by taking the depth-integrated transfer rates of Pomphrey et al. (1980), assuming $\dot{E} \propto N^2$ and normalizing to $N = 3$ cph. Although this accounts for the nominal buoyancy scaling of the energy transport rate, it does not account for variations in the distribution of $\dot{E}(m)$ associated with variations in N via $m_* = (N/N_o)\pi j_*/b$ in their model. Finally, their estimates of $\dot{E}(m)$ are arrived at by integrating only over regions of the spectral domain for which $\dot{E}(m,\omega)$ is negative.

b. Near-resonant interactions

Substantial motivation for this work is the question of whether the GM76 spectrum (Cairns and Williams 1976) represents a stationary state. We have seen that numerical evaluations of a resonant kinetic equation return $O(1)$ normalized Boltzmann rates and hence we are led to conclude that GM76 is not a stationary state with respect to resonant interactions. The next natural question to ask is whether the GM76 could be a stationary solution of the kinetic equation with the self-consistent broadening function $\gamma_{\mathbf{p}}$.

Our investigation of this question is currently limited by the absence of an iterative solution to (30) and (32) and consequent choice to parameterize the resonance broadening in terms of (34). As we go from nearly resonant evaluations (10^{-3} and 10^{-2}) to incorporating significant broadening (10^{-1} and 0.5), we find a significant decreases in the normalized Boltzmann rate. The largest decreases are associated with an expanded region of energy loss associated the parametric subharmonic instability, in which minimum normalized Boltzmann rates change from −3.38 to −0.45 at $(\omega, mb/2\pi) = (2.5f, 150)$. Large decreases here are not surprising given the sharp boundary between regions of loss and gain in the resonant calculations. Smaller changes are noted within the induced diffusion regime. Maximum normalized Boltzmann rates change from 2.6 to 1.5 at $(\omega, mb/2\pi) = (8f, 260)$. Broadening of the resonances to exceed the boundaries of the spectral domain could be making a contribution to such changes.

We regard our calculations here as a preliminary step to answering the question of whether the GM76 spectrum represents a stationary state with respect to nonlinear interactions within wave turbulence methodology. Complementary studies could include comparison with analyses of numerical solutions of the equations of motion.

7. Discussion

a. Resonant interactions

Several loose ends need to be tied up regarding the assertion that the GM76 spectrum does not constitute a stationary state with respect to resonant interactions. The first is the interpretation of McComas and Müller's (1981a) inertial-range theory with constant downscale transfer of energy. This constant downscale transfer of energy was obtained by patching together the induced diffusion and parametric subharmonic instability mechanisms and is attended by the following caveats: First, the inertial-subrange solution is found only after integrating over the frequency domain and numerical evaluations of the kinetic equation demonstrate that the inertial-subrange

[4] A potential interpretation is that this net energy flow out of the nonequilibrium part of the spectrum represents the energy requirements to maintain the spectrum.

solution also requires dissipation to balance energy gain at high vertical wavenumber. It takes significant effort to analyze their figures to understand how figures in McComas and Müller (1981a) plots relate to the initial tendency estimates in Fig. 5. Second, Pomphrey et al. (1980) argue that GM76 is a near-equilibrium state because of a one to three order of magnitude cancellation between the Langevin rates in the induced diffusion regime. However, this is just the ω^2/f^2 difference between the fast and slow induced diffusion time scales. It does not imply small values of the slow induced diffusion time scale, which are equivalent to the normalized Boltzmann rates. Third, the large normalized Boltzmann rates determined by our numerical procedure are associated with the elastic scattering mechanism rather than induced diffusion. Normalized Boltzmann rates for the induced diffusion and elastic scattering mechanisms are

$$\epsilon_{\rm id} = \frac{\pi^2}{20}\frac{m}{m_c}\frac{m^2}{m^2 + m_*^2\dfrac{\omega^2}{f^2}} \quad \text{and}$$

$$\epsilon_{\rm es} = \frac{\pi^2}{20}\frac{m}{m_c}\frac{m^2}{m^2 + 0.25m_*^2},$$

in which m_* represents the low-wavenumber rolloff of the vertical wavenumber spectrum (vertical mode-3 equivalent here); m_c is the high-wavenumber cutoff, nominally at 10-m wavelengths; and the GM76 spectrum has been assumed. The normalized Boltzmann rates for ES and ID are virtually identical at high wavenumber. They differ only in how their respective triads connect to the $\omega = f$ boundary. Induced diffusion connects along a curve whose resonance condition is approximately that the high-frequency group velocity match the near-inertial vertical phase speed, $\omega/m = f/m_{ni}$. Elastic scattering connects along a simpler $m = 2m_{ni}$. Evaluations of the kinetic equation reveal nearly vertical contours throughout the vertical wavenumber domain, consistent with ES, rather than sloped along contours of $\omega \propto m$ emanating from $m = m_*$ as expected with the ID mechanism.

The identification of the ES mechanism as being responsible for the large normalized Boltzmann rates at high vertical wavenumber requires further explanation. The role assigned to the ES mechanism by McComas and Bretherton (1977) is the equilibration of a vertically anisotropic field. This can be seen by taking the near-inertial component of a triad to represent $\mathbf{p}_1$, assuming that the action density of the near-inertial field is much larger than the high-frequency fields, and taking the limit $(k, l, m) = (k_2, l_2, -m_2) \equiv \mathbf{p}^-$. Thus,

$$f_{p12} = n_{\mathbf{p}_1} n_{\mathbf{p}_2} - n_{\mathbf{p}}(n_{\mathbf{p}_1} + n_{\mathbf{p}_2}) \cong n_{\mathbf{p}_1}[n_{\mathbf{p}^-} - n_{\mathbf{p}}],$$

and transfers proceed until the field is isotropic, $n_{\mathbf{p}^-} = n_{\mathbf{p}}$. However, this is not the complete story. A more precise characterization of the resonance surface takes into account the frequency resonance requiring $\omega - \omega_2 = \omega_1 \cong f$ and requires $O(\omega/f)$ differences in m and $-m_2$ if $k = k_2$ and $O(\omega/f)$ differences in k and k_2 if $m = -m_2$. For an isotropic field,

$$f_{p12} = n_{\mathbf{p}_1} n_{\mathbf{p}_2} - n_{\mathbf{p}}(n_{\mathbf{p}_1} + n_{\mathbf{p}_2}) \cong n_{p_1}[n_{\mathbf{p}+\delta\mathbf{p}} - n_{\mathbf{p}}] \cong n_{\mathbf{p}_1}[\delta\mathbf{p} \cdot \nabla n_{\mathbf{p}}],$$

with $\delta\mathbf{p} = \mathbf{p}_2 - \mathbf{p}$.

b. *Near-resonant interactions*

The idea of trying to self-consistently find the smearing of the delta functions is not new. For internal waves, it appears in DeWitt and Wright (1982), Carnevale and Frederiksen (1983), and DeWitt and Wright (1984).

DeWitt and Wright (1982) set up a general framework for a self-consistent calculation similar in spirit to Lvov et al. (1997), using a path-integral formulation of the diagrammatic technique. DeWitt and Wright (1982) make an uncontrolled approximation that the nonlinear frequency renormalization $\Sigma(\mathbf{p}, \omega)$ is independent of ω and show that this assumption is not self-consistent. Lvov et al. (1997) present a more sophisticated approach to a self-consistent approximation to the operator $\Sigma(\mathbf{p}, \omega)$. In particular, DeWitt and Wright (1982) suggest

$$\Sigma(\mathbf{p}, \omega) = \Sigma(\mathbf{p}, \omega_{\mathbf{p}}),$$

whereas Lvov et al. (1997) propose a more self-consistent

$$\Sigma(\mathbf{p}, \omega) = \Sigma[\mathbf{p}, \omega_{\mathbf{p}} + i\Im\Sigma(\mathbf{p}, \omega_{\mathbf{p}})].$$

DeWitt and Wright (1984) evaluate the self-consistency of the resonant interaction approximation and find that, for high frequency and high wavenumbers, the resonant interaction representation is not self-consistent. A possible critique of these papers is that they use resonant matrix elements given by Müller and Olbers (1975) without appreciating that those elements can only be used strictly on the resonant manifold.

Carnevale and Frederiksen (1983) present similar expressions for two-dimensional stratified internal waves. There the kinetic equation is (7.4) with the triple correlation time given by Θ (our $\mathcal{L}$) of their (8.7).

The main advantage of our approach over Carnevale and Frederiksen (1983) is that we use systematic Hamiltonian structures that are equivalent to the primitive equations of motion rather than a simplified two-dimensional model.

c. *Direct numerical simulations of the dynamical equations of motion*

Direct numerical simulations of the dynamical equations of motion are not limited by the dynamical assumptions inherent in the weakly nonlinear resonant or near-resonant representations. They are however subject to other computational restrictions and do significantly depend upon details of forcing.

D'Asaro (1997) present spindown simulations based upon the GM76 spectrum with varying amplitude. The domain considered there consists of a rectangular box 80 km $\times$ 10 km $\times$ 1 km on a side with resolved wavelengths of 1 km in the horizontal and 50 m in the vertical. Note that this domain does not include regions in Fig. 5 exhibiting large values of the normalized Boltzmann rate. Interactions in the resolved domain may be dominated by PSI transfers as discussed in McComas and Müller (1981a).

Forced nonrotating simulations are presented in Furue (2003). The computational domain is a box of horizontal size 100 m $\times$ 100 m $\times$ 128 m height. The forcing is isotropic in wavenumber and peaks at a horizontal wavelength of 25 m. The forcing is controlled so that amplitudes are consistent with GM76 and the resulting dissipation is a significant fraction of that associated with GM76.

It is an interesting task for the future research to relate these numerical simulations with evaluations of the kinetic equations we are performing here. The first steps in this direction were performed in Lvov and Yokoyama (2009).

8. Conclusions

Our fundamental result is that the GM spectrum is not stationary with respect to the resonant interaction approximation. This result is contrary to the point of view expressed in McComas and Müller (1981a) and Müller et al. (1986) and gave us cause to review published results concerning resonant internal wave interactions. We also arrived at the point where we can say that the resonant kinetic equation does not constitute a self-consistent approach. We then included near-resonant interactions and found significant reductions in the temporal evolution of the GM spectrum.

This is the first step in building a self-consistent theory of the interactions of internal waves. The main point of this paper is that we reopen the challenge of how to calculate from first principles the spectral energy density of internal waves.

We compared the interaction matrices for three different Hamiltonian formulations and one non-Hamiltonian formulation in the resonant limit. Two of the Hamiltonian formulations are canonical and one (Lvov and Tabak 2004) avoids a linearization of the Hamiltonian prior to assuming an expansion in terms of weak nonlinearity. Formulations in Eulerian, isopycnal, and Lagrangian coordinate systems were considered. All four representations lead to equivalent results on the resonant manifold in the absence of background rotation. The two representations that include background rotation, a canonical Hamiltonian formulation in isopycnal coordinates and a noncanonical Hamiltonian formulation in Lagrangian coordinates, also lead to equivalent results on the resonant manifold. This statement is not trivial given the different assumptions and coordinate systems that have been used for the derivation of the various kinetic equations. It points to an internal consistency on the resonant manifold that we still do not completely understand and appreciate.

We rationalize the consistent results as being associated with potential vorticity conservation. In the isopycnal coordinate canonical Hamilton formulation, potential vorticity conservation is explicit. In the Lagrangian coordinate noncanonical Hamiltonian, potential vorticity conservation results from a projection onto the linear modes of the system. The two nonrotating formulations prohibit relative vorticity variations by casting the velocity as the gradient of a scalar streamfunction.

We infer that the nonstationary results for the GM spectrum are related to a higher-order approximation of the elastic scattering mechanism than considered in McComas and Bretherton (1977) and McComas and Müller (1981b). Our numerical results indicate evolution rates of an inverse wave period at high vertical wavenumber, signifying a system that is not weakly nonlinear. To understand whether such nonweak conditions could give rise to competing effects that render the system stationary, we considered resonance broadening. We used a kinetic equation with broadened frequency delta function derived for a generalized three-wave Hamiltonian system in (Lvov et al. 1997). The derivation is based upon the Wyld diagrammatic technique for nonequilibrium wave systems and utilizes the Dyson–Wyld line resummation. This broadened kinetic equation is perceived to be more sophisticated than the two-dimensional direct interaction approximation representation pursued in Carnevale and Frederiksen (1983) and the self-consistent calculations of DeWitt and Wright (1984), which utilized the resonant interaction matrix of Olbers (1976). We find a tendency of resonance broadening to lead to more stationary conditions. However, our results are limited by an uncontrolled approximation concerning the width of the resonance surface.

Reductions in the temporal evolution of the internal wave spectrum at high vertical wavenumber were greatest

for those frequencies associated with the PSI mechanism: that is, $f < \omega < 5f$. Smaller reductions were noted at high frequencies.

A common theme in the development of a kinetic equation is a perturbation expansion permitting the wave interactions and evolution of the spectrum on a slow time scale (e.g., section 2b). An assumption of Gaussian statistics at zeroth order permits a solution of the first-order triple correlations in terms of the zeroth-order quadruple correlations. Assessing the adequacy of this assumption for the zeroth-order high-frequency wave field is a challenge for future efforts. Such departures from Gaussianity could have implications for the stationarity at high frequencies.

Nontrivial aspects of our work are that we utilize the canonical Hamiltonian representation of Lvov and Tabak (2004), which results in a kinetic equation without first linearizing to obtain interaction coefficients defined only on the resonance surface and the sophisticated broadened closure scheme of Lvov et al. (1997). Inclusion of interactions between internal waves and modes of motion associated with zero eigenfrequency (i.e., the vortical motion field) is a challenge for future efforts.

We found no coordinate-dependent (i.e., Eulerian, isopycnal, or Lagrangian) differences between interaction matrices on the resonant surface. We regard it as intuitive that there will be coordinate-dependent differences off the resonant surface. It is a robust observational fact that Eulerian frequency spectra at high vertical wavenumber are contaminated by vertical Doppler shifting: near-inertial frequency energy is Doppler shifted to higher frequency at approximately the same vertical wavelength. Use of an isopycnal coordinate system considerably reduces this artifact (Sherman and Pinkel 1991). Further differences are anticipated in a fully Lagrangian coordinate system (Pinkel 2008). Thus, differences in the approaches may represent physical effects and what is a stationary state in one coordinate system may not be a stationary state in another. Obtaining canonical coordinates in an Eulerian coordinate system with rotation and in the Lagrangian coordinate system are challenges for future efforts. In conclusion, the purpose of this paper is to show that the first principle explanation of internal wave spectrum in general and Garrett and Munk in particular are still yet to come.

Acknowledgments. YL is supported by NSF DMS Grant 0807871 and ONR Award N00014-09-1-0515. We are grateful to YITP in Kyoto University for permitting use of their facility.

APPENDIX

Historical Review of Other Matrix Elements

Our attention is restricted to the hydrostatic balance case, for which

$$|\mathbf{k}| \ll |m|. \tag{A1}$$

A minor detail is that the linear frequency has different algebraic representations in isopycnal and Cartesian coordinates. The Cartesian vertical wavenumber k_z and the density wavenumber m are related as $m = -g/(\rho_0 N^2)k_z$, where g is gravity, ρ is density with reference value ρ_0, N is the buoyancy (Brunt–Väisälä) frequency, and f is the Coriolis frequency. In isopycnal coordinates, the dispersion relation is given by

$$\omega(\mathbf{p}) = \sqrt{f^2 + \frac{g^2}{\rho_0^2 N^2}\frac{|\mathbf{k}|^2}{m^2}}. \tag{A2}$$

In Cartesian coordinates,

$$\omega(\mathbf{p}) = \sqrt{f^2 + N^2\frac{|\mathbf{k}|^2}{k_z^2}}. \tag{A3}$$

In the limit of $f = 0$, these dispersion relations assume the form

$$\omega_{\mathbf{p}} \propto \frac{|\mathbf{k}|}{|m|} \propto \frac{|\mathbf{k}|}{|k_z|}. \tag{A4}$$

a. *Hamiltonian formalism in Clebsch variables in Voronovich (1979)*

Voronovich starts from the nonrotating equations in Eulerian coordinates,

$$\begin{aligned} \frac{\partial \mathbf{u}}{\partial t} + \mathbf{u}\cdot\nabla\mathbf{u} &= \frac{-1}{\rho}\nabla p - g\mathbf{z} \\ \nabla\cdot\mathbf{u} &= 0 \\ \frac{\partial \rho}{\partial t} + \mathbf{u}\cdot\nabla\rho &= 0, \end{aligned} \tag{A5}$$

with unit vector $\mathbf{z}$ defining the vertical direction. The Hamiltonian of the system is

$$\mathcal{H} = \int\left[(\rho_0 + \rho)\frac{\mathbf{v}^2}{2} + \Pi(\rho_o + \rho) - \Pi(\rho_o) + \rho g z\right]d\mathbf{r}, \tag{A6}$$

where $\rho_0(z)$ is the equilibrium density profile; ρ is the wave perturbation; and Π is a potential energy density function,

$$\Pi(\rho_o + \rho) - \Pi(\rho_o) + \rho g z = g\int_{\eta(\rho_o+\rho)}^{\eta(\rho_o)} [\rho_0 + \rho - \rho_0(\xi)]\, d\xi, \tag{A7}$$

with $\eta(\xi)$ being the inverse of $\rho_o(z)$. The intent is to use ρ and Lagrange multiplier λ as the canonically conjugated Hamiltonian pair,

$$\dot{\lambda} = \frac{\partial \mathcal{H}}{\partial \rho} = -(\mathbf{v}\nabla)\lambda + g[z - \eta(\rho_o + \rho)] \quad \text{and} \tag{A8}$$

$$\dot{\rho} = -\frac{\partial \mathcal{H}}{\partial \lambda} = -(\mathbf{v}\nabla)(\rho_o + \rho), \tag{A9}$$

with $z - \eta(\rho_o + \rho)$ being the vertical displacement of a fluid parcel and the second equation representing continuity. The issue is to express the velocity $\mathbf{v}$ as a function of λ and ρ, and to this end one introduces yet another function Φ with the harmonious feature

$$\frac{\delta \mathcal{H}}{\delta \Phi} = 0 \tag{A10}$$

and a constraint. That constraint is provided by

$$\nabla \cdot \mathbf{v} = -\frac{\delta \mathcal{H}}{\delta \Phi} = 0. \tag{A11}$$

Voronovich (1979) then identifies the functional relationship

$$\mathbf{v} = \frac{1}{\rho_0 + \rho}[\nabla\Phi + \lambda\nabla(\rho_0 + \rho)] \cong \frac{1}{\rho}[\nabla\Phi + \lambda\nabla(\rho_0 + \rho)], \tag{A12}$$

with the right-hand side representing the Boussinesq approximation. The only thing stopping progress at this point is the explicit appearance of ξ in (A7), and to eliminate this explicit dependence a Taylor series in density perturbation ρ relative to ρ_0 is used to express the potential energy in terms of ρ and λ. The resulting Hamiltonian $\mathcal{H}$ is

$$\mathcal{H} = \int\left[\frac{v^2}{2} + \Pi(\rho_o + \rho) - \Pi(\rho_o) + \rho g z\right] d\mathbf{r} \cong \frac{1}{2}\int\left\{\lambda\nabla(\rho_o + \rho)[\nabla\Phi + \lambda\nabla(\rho_o + \rho)] - \frac{g}{\rho_o'}\rho^2 + \frac{g\rho_o''}{\rho_o'^3}\frac{\rho^3}{3}\right\} d\mathbf{r}, \tag{A13}$$

with primes indicating $\partial/\partial z$.

The only approximations that have been made to obtain (A13) are the Boussinesq approximation in the nonrotating limit, the specification that the velocity be represented as (A12), and a Taylor series expansion. The Taylor series expansion is used to express the Hamiltonian in terms of canonically conjugated variables ρ and λ. Truncation of this Taylor series is the essence of the slowly varying approximation that the vertical scale of the internal wave is smaller than the vertical scale of the background stratification, which requires, for consistency's sake, the hydrostatic approximation.

The procedure of introducing additional functionals (Φ) and constraints [(A11)] originates in Clebsch (1859). See Seliger and Witham (1968) for a discussion of Clebsch variables and also section 7.1 of Miropolsky (1981).

Finally, the evolution equation for wave amplitude $a_{\mathbf{p}}$ is produced by expressing the cubic terms in the Hamiltonian with solutions to the linear problem represented by the quadratic components of the Hamiltonian. This is an explicit linearization of the problem prior to the formulation of the kinetic equation.

Specifically, we formulate the matrix elements for Voronovich's Hamiltonian using his equation (A.1). This formula is derived for general boundary conditions. To compare with other matrix elements of this paper, we assume a constant stratification profile and Fourier basis as the vertical structure function $\phi(z)$. That allows us to solve for the matrix elements defined via (11) and above it in his paper. Then the convolutions of the basis functions give delta functions in vertical wavenumbers. Vornovich's (A.1) transforms into

$$\begin{aligned}|V^{\mathbf{p}}_{\mathbf{p}_1,\mathbf{p}_2}{}^{\mathrm{V}}|^2 \propto \frac{|\mathbf{k}||\mathbf{k}_1||\mathbf{k}_2|}{|mm_1m_2|}\Bigg\{ & -m\left[\frac{1}{|\mathbf{k}||m|}\left(\frac{\mathbf{k}\cdot\mathbf{k}_1|m_1|}{|\mathbf{k}_1|} + \frac{\mathbf{k}\cdot\mathbf{k}_2|m_2|}{|\mathbf{k}_2|}\right) + \frac{\omega_1 + \omega_2 - \omega}{\omega}\right] \\ & + m_1\left[\frac{1}{|\mathbf{k}_1||m_1|}\left(\frac{\mathbf{k}\cdot\mathbf{k}_1|m|}{|\mathbf{k}|} + \frac{\mathbf{k}_1\cdot\mathbf{k}_2|m_2|}{|\mathbf{k}_2|}\right) - \frac{\omega_1 + \omega_2 - \omega}{\omega_1}\right] \\ & + m_2\left[\frac{1}{|\mathbf{k}_2||m_2|}\left(\frac{\mathbf{k}\cdot\mathbf{k}_2|m|}{|\mathbf{k}|} + \frac{\mathbf{k}_2\cdot\mathbf{k}_1|m_1|}{|\mathbf{k}_1|}\right) - \frac{\omega_1 + \omega_2 - \omega}{\omega_2}\right]\Bigg\}^2.\end{aligned} \tag{A14}$$

Note that Eq. (A14) shares structural similarities with the interaction matrix elements in isopycnal coordinates, Eq. (A22) below.

b. Olbers, McComas, and Meiss

Derivations presented in Olbers (1974), McComas (1975), and Meiss et al. (1979) are based upon the Lagrangian equations of motion,

$$\ddot{x}_1 - f\dot{x}_2 = \frac{-1}{\rho}p_{x_1}, \quad \ddot{x}_2 + f\dot{x}_1 = \frac{-1}{\rho}p_{x_2},$$
$$\ddot{x}_3 + g = \frac{-1}{\rho}p_{x_3}, \quad \partial(x_1,x_2,x_3)/\partial(r_1,r_2,r_3) = 1, \qquad \text{(A15)}$$

expressing momentum conservation and incompressibility. Here, $\mathbf{r}$ is the initial position of a fluid parcel at $\mathbf{x}$: these are Lagrangian coordinates. In the context of Hamiltonian mechanics, the associated Lagrangian density is

$$\mathcal{L} = \frac{1}{2}\rho(\dot{x}_i\dot{x}_j + \epsilon_{jkl}f_i\dot{x}_k x_l) - \rho g\delta_{j3}x_j + \mathcal{P}(J-1),$$

where $x_j = x_j(\mathbf{r}, t)$ is the instantaneous position of the parcel of fluid, which was initially at $\mathbf{r}$; $\mathcal{P}(\mathbf{x})$ is a Lagrange multiplier corresponding to pressure; and $J = \partial\mathbf{x}/\partial\mathbf{r}$ is the Jacobian, which ensures the fluid is incompressible.

In terms of variables representing a departure from hydrostatic equilibrium,

$$\xi_j(\mathbf{r},t) = x_j(\mathbf{r},t) - r_j, \quad \pi(\mathbf{r},t) = P(\mathbf{x},t) - \mathcal{P}_k(\mathbf{r}),$$

the Boussinesq Lagrangian density $\mathcal{L}$ for slow variations in background density ρ is

$$\mathcal{L} = \frac{1}{2}\left[\xi_i^2 + \epsilon_{jkl}f_i\dot{\xi}_k\xi_l - N^2\xi_3^2 + \pi\left(\frac{\partial\xi_i}{\partial x_i} + \Delta_{ii} + \Delta\right)\right], \qquad \text{(A16)}$$

with $\partial\xi_i/\partial x_i + \Delta_{ii} + \Delta$ representing the continuity equation where $\Delta = \det(\partial\xi_i/\partial x_j)$.

This Lagrangian is then projected onto a single wave amplitude variable a using the linear internal wave consistency relations[A1] based upon plane wave solutions [e.g., Müller 1976, (2.26)], and a perturbation expansion in wave amplitude is proposed. This process has two consequences: the use of internal wave consistency relations places a condition of zero perturbation potential vorticity upon the result, and the expansion places a small-amplitude approximation upon the result with ill-defined domain of validity relative to the (later) assertion of weak interactions.

The evolution equation for wave amplitude is Lagrange's equation,

$$\frac{d}{dt}\frac{\partial\mathcal{L}}{\partial\dot{a}_0} - \frac{\partial\mathcal{L}}{\partial a_0} = 0, \qquad \text{(A17)}$$

in which a_0 is the zeroth-order wave amplitude. After a series of approximations, this equation is cast into a field variable equation similar to (10). We emphasize that to get there small displacement of parcel of fluid was used, together with the built in assumption of resonant interactions between internal wave modes. The Lvov and Tabak (2001, 2004) approach is free from such limitations.

Specifically, matrix elements derived in Olbers (1974) are given by $|V^{\mathbf{p}\ \mathrm{MO}}_{\mathbf{p}_2,\mathbf{p}}|^2 = T^+/(4\pi)$ and $|V^{\mathbf{p}_1\ \mathrm{MO}}_{\mathbf{p}_2,\mathbf{p}}|^2 = T^-/(4\pi)$. We extracted $T^{\pm}$ from the appendix of Müller and Olbers (1975). In our notation, in the hydrostatic balance approximation, their matrix elements are given by

$$|V^{\mathbf{p}\ \mathrm{MO}}_{\mathbf{p}_1,\mathbf{p}_2}|^2 = \frac{(N_0^2 - f^2)^2}{32\rho_0}\omega\omega_1\omega_2\left|\frac{|\mathbf{k}||\mathbf{k}_1||\mathbf{k}_2|}{\omega\omega_1\omega_2|\mathbf{p}||\mathbf{p}_1||\mathbf{p}_2|}\right.$$
$$\times\left[-\frac{\left(-m_1\dfrac{\mathbf{k}_1\cdot\mathbf{k}_2 - if\mathbf{k}_2\cdot\mathbf{k}_1^{\perp}/\omega_1}{k_1^2} + m_2\right)\left(-m_2\dfrac{\mathbf{k}_1\cdot\mathbf{k}_2 - if\mathbf{k}_1\cdot\mathbf{k}_2^{\perp}/\omega_2}{k_2^2} + m_1\right)}{m}\right.$$
$$-\frac{\left(-m_2\dfrac{\mathbf{k}_2\cdot\mathbf{k} + if\mathbf{k}_2\cdot\mathbf{k}^{\perp}/\omega_2}{k_2^2} + m\right)\left(-m\dfrac{\mathbf{k}_2\cdot\mathbf{k} - if\mathbf{k}\cdot\mathbf{k}_2^{\perp}/\omega}{k^2} + m_2\right)}{m_1}$$
$$\left.\left.-\frac{\left(-m\dfrac{\mathbf{k}\cdot\mathbf{k}_1 - if\mathbf{k}\cdot\mathbf{k}_1^{\perp}/\omega}{k^2} + m_1\right)\left(-m_1\dfrac{\mathbf{k}\cdot\mathbf{k}_1 + if\mathbf{k}_1\cdot\mathbf{k}^{\perp}/\omega_1}{k_1^2} + m\right)}{m_2}\right]\right|^2. \qquad \text{(A18)}$$

Taking an $f = 0$ limit reduces the problem to a scale-invariant problem. We get the following simplified expression:

[A1] Wave amplitude a is defined so that a^*a is proportional to wave energy.

$$|V^{\mathbf{p}\ \mathrm{MO}}_{\mathbf{p}_1,\mathbf{p}_2}|^2 \propto \frac{|\mathbf{k}||\mathbf{k}_1||\mathbf{k}_2|}{|mm_1m_2|}\left[-\frac{1}{m}\left(-\frac{m_2\mathbf{k}_1\cdot\mathbf{k}_2}{|\mathbf{k}_2|^2}+m_1\right)\left(-\frac{m_1\mathbf{k}_2\cdot\mathbf{k}_1}{|\mathbf{k}_1|^2}+m_2\right)+\frac{1}{m_1}\left(\frac{m_2\mathbf{k}\cdot\mathbf{k}_2}{|\mathbf{k}_2|^2}-m\right)\left(-\frac{m\mathbf{k}_2\cdot\mathbf{k}}{|\mathbf{k}|^2}+m_2\right)\right.$$
$$\left.+\frac{1}{m_2}\left(-\frac{m\mathbf{k}_1\cdot\mathbf{k}}{|\mathbf{k}|^2}+m_1\right)\left(\frac{m_1\mathbf{k}\cdot\mathbf{k}_1}{|\mathbf{k}_1|^2}-m\right)\right]^2. \tag{A19}$$

This simplified expression is going to be used for comparison of approaches in section 3.

c. Caillol and Zeitlin

A non-Hamiltonian kinetic equation for internal waves was derived in Caillol and Zeitlin (2000), their (61), directly from the dynamical equations of motion, without the use of the Hamiltonian structure. Caillol and Zeitlin (2000) invoke the Craya–Herring decomposition for nonrotating flows, which enforces a condition of zero perturbation vorticity on the result.

To make it appear equivalent to more traditional form of kinetic equation, as in Zakharov et al. (1992), we make a change of variables, $\mathbf{l} \to -\mathbf{l}$ in the second line and $\mathbf{k} \to -\mathbf{k}$ in the third line of (61) of Caillol and Zeitlin (2000). If we further assume that all spectra are symmetric, $n(-\mathbf{p}) = n(\mathbf{p})$, then the kinetic equation assumes traditional form, as in Eq. (22) (see Müller and Olbers 1975; Zakharov et al. 1992; Lvov and Tabak 2001, 2004).

The matrix elements according to Caillol and Zeitlin (2000) are shown as $X_{k,l,p}$ and $Y^{\pm}_{k,l,p}$ in their (62) and (63), where $|V^{\mathbf{p}\ \mathrm{CZ}}_{\mathbf{p}_1,\mathbf{p}_2}|^2 = X_{\mathbf{p}_1,\mathbf{p}_2,\mathbf{p}}$ and $|V^{\mathbf{p}_1\ \mathrm{CZ}}_{\mathbf{p}_2,\mathbf{p}}|^2 = Y^{+}_{\mathbf{p}_1,-\mathbf{p}_2,\mathbf{p}}$. In our notation, it reads as

$$|V^{\mathbf{p}\ \mathrm{CZ}}_{\mathbf{p}_1,\mathbf{p}_2}|^2 \propto [|\mathbf{k}|\mathrm{sgn}(m)+|\mathbf{k}_1|\mathrm{sgn}(m_1)+|\mathbf{k}_2|\mathrm{sgn}(m_2)]^2\frac{(m^2-m_1m_2)^2}{|m||m_1||m_2||\mathbf{k}||\mathbf{k}_1||\mathbf{k}_2|}$$
$$\times\left[\frac{|\mathbf{k}|^2-|\mathbf{k}_1|\mathrm{sgn}(m_1)|\mathbf{k}_2|\mathrm{sgn}(m_2)}{m^2-m_1m_2}m-\frac{|\mathbf{k}_1|^2}{m_1}-\frac{|\mathbf{k}_2|^2}{m_2}\right]^2. \tag{A20}$$

This expression is going to be used for comparison of approaches in section 3.

d. Kenyon and Hasselmann

The first kinetic equations for wave–wave interactions in a continuously stratified ocean appear in Kenyon (1966), Hasselmann (1966), and Kenyon (1968). Kenyon (1968) states (without detail) that Kenyon (1966) and Hasselmann (1966) give numerically similar results. We have found that Kenyon (1966) differs from the four approaches examined below on one of the resonant manifolds but have not pursued the question further. It is possible this difference results from a typographical error in Kenyon (1966). We have not rederived this non-Hamiltonian representation and thus exclude it from this study.

e. Pelinovsky and Raevsky

An important paper on internal waves is Pelinovsky and Raevsky (1977). Clebsch variables are used to obtain the interaction matrix elements for both constant stratification rates, N = constant, and arbitrary buoyancy profiles, $N = N(z)$, in a Lagrangian coordinate representation. Not many details are given, but there are some similarities in appearance with the Eulerian coordinate representation of Voronovich (1979). The most significant result is the identification of a scale-invariant (nonrotating and hydrostatic) stationary state, which we refer to as the Pelinovsky–Raevsky in the companion paper (Lvov et al. 2010). It is stated in Pelinovsky and Raevsky (1977) that their matrix elements are equivalent to those derived in their citation [11], which is Brehovski (1975). Because Brehovski (1975) and Pelinovsky and Raevsky (1977) are in Russian and not generally available, we refrain from including them in this comparison.

f. Milder

An alternative Hamiltonian description was developed in Milder (1982), in isopycnal coordinates without assuming a hydrostatic balance. The resulting Hamiltonian is an iterative expansion in powers of a small parameter, similar to the case of surface gravity waves. In principle, that approach may also be used to calculate wave–wave interaction amplitudes. Because those calculations were not done in Milder (1982), we do not pursue the comparison further.

g. Isopycnal Hamiltonian

Finally, in Lvov and Tabak (2004) the following wave–wave interaction matrix element was derived based on a canonical Hamiltonian formulation in isopycnal coordinates:

$$|V^{0\,\mathrm{H}}_{1,2}|^2 = \frac{N^2}{32g}\left\langle\left(\frac{k\mathbf{k}_1\cdot\mathbf{k}_2}{k_1k_2}\sqrt{\frac{\omega_1\omega_2}{\omega}} + \frac{k_1\mathbf{k}_2\cdot\mathbf{k}}{k_2k}\sqrt{\frac{\omega_2\omega}{\omega_1}} + \frac{k_2\mathbf{k}\cdot\mathbf{k}_1}{kk_1}\sqrt{\frac{\omega\omega_1}{\omega_2}} + \frac{f^2}{\sqrt{\omega\omega_1\omega_2}}\frac{k_1^2\mathbf{k}_2\cdot\mathbf{k} - k_2^2\mathbf{k}\cdot\mathbf{k}_1 - k^2\mathbf{k}_1\cdot\mathbf{k}_2}{kk_1k_2}\right)^2 + \left\{f\frac{\mathbf{k}_1\cdot\mathbf{k}_2^{\perp}}{kk_1k_2}\left[\sqrt{\frac{\omega}{\omega_1\omega_2}}(k_1^2 - k_2^2) - \sqrt{\frac{\omega_1}{\omega_2\omega}}(k_2^2 - k^2) - \sqrt{\frac{\omega_2}{\omega\omega_1}}(k^2 - k_1^2)\right]\right\}^2\right\rangle. \tag{A21}$$

Lvov and Tabak (2001) is a rotationless limit of Lvov and Tabak (2004). Taking the $f \to 0$ limit, Lvov and Tabak (2004) reduces to Lvov and Tabak (2001) and (A21) reduces to

$$|V^{\mathbf{p}\ \mathrm{H}}_{\mathbf{p}_1,\mathbf{p}_2}|^2 \propto \frac{1}{|\mathbf{k}||\mathbf{k}_1||\mathbf{k}_2|}\left(|\mathbf{k}|\mathbf{k}_1\cdot\mathbf{k}_2\sqrt{\left|\frac{m}{m_1m_2}\right|} + |\mathbf{k}_1|\mathbf{k}_2\cdot\mathbf{k}\sqrt{\left|\frac{m_1}{m_2m}\right|} + |\mathbf{k}_2|\mathbf{k}\cdot\mathbf{k}_1\sqrt{\left|\frac{m_2}{mm_1}\right|}\right)^2. \tag{A22}$$

Observe that, in this form, these equations share structural similarities with (A14).

REFERENCES

Annenkov, S., and V. I. Shrira, 2006: Role of non-resonant interactions in the evolution of nonlinear random water wave fields. *J. Fluid Mech.,* **561,** 181–207.

Brehovski, L. M., 1975: On interactions of internal and surface waves in the ocean. *Oceanology,* **15,** 205–212.

Caillol, P., and V. Zeitlin, 2000: Kinetic equations and stationary energy spectra of weakly nonlinear internal gravity waves. *Dyn. Atmos. Oceans,* **32,** 81–112.

Cairns, J. L., and G. O. Williams, 1976: Internal wave observations from a midwater float. *2. J. Geophys. Res.,* **81,** 1943–1950.

Carnevale, G. F., and J. S. Frederiksen, 1983: A statistical dynamical theory of strongly nonlinear internal gravity waves. *Geophys. Astrophys. Fluid Dyn.,* **23,** 175–207.

Clebsch, A., 1859: Über die Integration der hydrodynamischen Gleichungen (in German). *J. Reine Angew. Math.,* **56,** 1–10.

D'Asaro, W., 1997: Direct simulation of internal wave energy transfer. *J. Phys. Oceanogr.,* **27,** 1937–1945.

DeWitt, R. J., and J. Wright, 1982: Self-consistent effective medium theory of random internal waves. *J. Fluid Mech.,* **115,** 283.

——, and ——, 1984: Self-consistent effective medium parameters for oceanic internal waves. *J. Fluid Mech.,* **146,** 252.

Furue, R., 2003: Energy transfer within the small-scale oceanic internal wave spectrum. *J. Phys. Oceanogr.,* **33,** 267–282.

Garrett, C. J. R., and W. H. Munk, 1972: Space-timescales of internal waves. *Geophys. Fluid Dyn.,* **2,** 225–264.

——, and ——, 1975: Space-timescales of internal waves. A progress report. *J. Geophys. Res.,* **80,** 291–297.

——, and ——, 1979: Internal waves in the ocean. *Annu. Rev. Fluid. Mech.,* **11,** 339–369.

Gershgorin, B., Y. V. Lvov, and D. Cai, 2007: Interactions of renormalized waves in thermalized Fermi-Pasta-Ulam chains. *Phys. Rev.,* **75,** 046603, doi:10.1103/PhysRevE.75.046603.

Hasselmann, K., 1966: Feynman diagrams and interaction rules of wave-wave scattering processes. *Rev. Geophys.,* **4,** 1–32.

Janssen, P. A. E. M., 2003: Nonlinear four-wave interactions and freak waves. *J. Phys. Oceanogr.,* **33,** 863–884.

Kenyon, K. E., 1966: Wave-wave scattering for gravity waves and Rossby waves. Ph.D. thesis, University of California, San Diego, 103 pp.

——, 1968: Wave-wave interactions of surface and internal waves. *J. Mar. Res.,* **26,** 208–231.

Kramer, P. R., J. A. Biello, and Y. V. Lvov, 2003: Application of weak turbulence theory to FPU model. *Proc. Fourth Int. Conf. on Dynamical Systems and Differential Equations,* Wilmington, NC, AIMS, 482–491.

Lelong, M.-P., and J. J. Riley, 1992: Internal wave-vortical mode interactions in strongly stratified flows. *J. Fluid Mech.,* **232,** 1–19.

——, and ——, 2000: Fluid motions in the presence of strong stable stratification. *Annu. Rev. Fluid Mech.,* **32,** 613–658.

Lvov, V. S., Y. V. Lvov, A. C. Newell, and V. E. Zakharov, 1997: Statistical description of acoustic turbulence. *Phys. Rev.,* **56E,** 390–405.

Lvov, Y. V., and E. G. Tabak, 2001: Hamiltonian formalism and the Garrett and Munk spectrum of internal waves in the ocean. *Phys. Rev. Lett.,* **87,** 168501, doi:10.1103/PhysRevLett.87.168501.

——, and S. Nazarenko, 2004: Noisy spectra, long correlations, and intermittency in wave turbulence. *Phys. Rev.,* **69E,** 066608, doi:10.1103/PhysRevE.69.066608.

——, and E. G. Tabak, 2004: A Hamiltonian formulation for long internal waves. *Physica D,* **195,** 106–122.

——, and N. Yokoyama, 2009: Energy spectra of internal waves in stratified fluid: Direct numerical simulations. *Physica D,* **238,** 803–815.

——, S. Nazarenko, and B. Pokorni, 2006: Discreteness and its effect on the water-wave turbulence. *Physica D,* **218,** 24–35.

——, K. L. Polzin, E. G. Tabak, and N. Yokoyama, 2010: Oceanic internal-wave field: Theory of scale-invariant spectra. *J. Phys. Oceanogr.,* **40,** 2605–2623.

McComas, C. H., 1975: Nonlinear interactions of internal gravity waves. Ph.D. thesis, The Johns Hopkins University, 113 pp.

——, 1977: Equilibrium mechanisms within the oceanic internal wavefield. *J. Phys. Oceanogr.,* **7,** 836–845.

——, and F. P. Bretherton, 1977: Resonant interaction of oceanic internal waves. *J. Geophys. Res.,* **82,** 1397–1412.

——, and P. Müller, 1981a: The dynamic balance of internal waves. *J. Phys. Oceanogr.,* **11,** 970–986.

——, and ——, 1981b: Time scales of resonant interactions among oceanic internal waves. *J. Phys. Oceanogr.,* **11,** 139–147.

Meiss, J. D., N. Pomphrey, and K. M. Watson, 1979: Numerical analysis of weakly nonlinear wave turbulence. *Proc. Natl. Acad. Sci. USA,* **76,** 2109–2113.

Milder, M., 1982: Hamiltonian description of internal waves. *J. Fluid Mech.,* **119,** 269–282.

Miropolsky, Y. Z., 1981: *Dinamika vnutrennih gravitacionnih voln v okeane*. Gidrometeroizdat, 302 pp.

Müller, P., 1976: On the diffusion of momentum and mass by internal gravity waves. *J. Fluid Mech.,* **77,** 789–823.

——, and D. J. Olbers, 1975: On the dynamics of internal waves in the deep ocean. *J. Geophys. Res.,* **80,** 3848–3860.

——, G. Holloway, F. Henyey, and N. Pomphrey, 1986: Nonlinear interactions among internal gravity waves. *Rev. Geophys.,* **24,** 493–536.

Olbers, D. J., 1974: On the energy balance of small scale internal waves in the deep sea. Hamburger Geophysikalische Einzelschriften 27, 91 pp.

——, 1976: Nonlinear energy transfer and the energy balance of the internal wave field in the deep ocean. *J. Fluid Mech.,* **74,** 375–399.

Pelinovsky, E. N., and M. A. Raevsky, 1977: Weak turbulence of internal waves in the ocean. *Izv. Atmos. Oceanic Phys.,* **13,** 187–193.

Pinkel, R., 2008: Advection, phase distortion, and the frequency spectrum of finescale fields in the sea. *J. Phys. Oceanogr.,* **38,** 291–313.

Pomphrey, N., J. D. Meiss, and K. D. Watson, 1980: Description of nonlinear internal wave interactions using langevin methods. *J. Geophys. Res.,* **85,** 1085–1094.

Seliger, R. L., and G. B. Witham, 1968: Variational principles in continuum mechanics. *Proc. Roy. Soc.,* **305A,** 1–25.

Sherman, J. T., and R. Pinkel, 1991: Estimates of the vertical wavenumber–frequency spectra of vertical shear and strain. *J. Phys. Oceanogr.,* **21,** 292–303.

Voronovich, A. G., 1979: Hamiltonian formalism for internal waves in the ocean. *Izv. Atmos. Oceanic Phys.,* **16,** 52–57.

Voronovich, V. V., I. A. Sazonov, and V. I. Shrira, 2006: On radiating solitons in a model of the internal wave shear flow resonance. *J. Fluid Mech.,* **568,** 273–301.

Yuen, H. C., and B. M. Lake, 1982: Nonlinear dynamics of deep-water gravity waves. *Adv. Appl. Mech.,* **22,** 67–229.

Zakharov, V. E., V. S. Lvov, and G. Falkovich, 1992: *Kolmogorov Spectra of Turbulence*. Springer-Verlag, 264 pp.